



## The biphasic effects of the oxLDL/ $\beta_2$ GPI/anti- $\beta_2$ GPI complex on VSMC proliferation and apoptosis

Ting Wang, Hong Zhou\*, Yudan Chen, Peng Zhang, Ting Wang

Department of Clinical Laboratory and Hematology, School of Medicine, Jiangsu University, Zhenjiang, Jiangsu 212013, China, Zhenjiang, Jiangsu 212013, PR China



### ARTICLE INFO

**Keywords:**  
oxLDL/ $\beta_2$ GPI/anti- $\beta_2$ GPI  
Proliferation  
Apoptosis  
Smooth muscle cell

### ABSTRACT

In our previous study, the oxLDL/ $\beta_2$ GPI/anti- $\beta_2$ GPI complex was demonstrated to further enhance the foam cell formation and migration of VSMC, as well as the expression of inflammatory cytokines, via the TLR4/NF- $\kappa$ B pathway. However, sparse information is available on other pro-atherogenic pathogenic effects of the oxLDL/ $\beta_2$ GPI/anti- $\beta_2$ GPI complex, such as effects on proliferation and apoptosis. In the present study, we focused on the biphasic effects and underlying mechanisms of the oxLDL/ $\beta_2$ GPI/anti- $\beta_2$ GPI complex on VSMC survival. The data showed that short exposure to the oxLDL/ $\beta_2$ GPI/anti- $\beta_2$ GPI complex could activate NF- $\kappa$ B and ERK1/2 pathways and stimulate cell proliferation in VSMC. In contrast, longer exposure increased the level of p38 pathway activation and cell apoptosis. Additionally, the promotion effect of the oxLDL/ $\beta_2$ GPI/anti- $\beta_2$ GPI complex on both proliferation and apoptosis, as well as signaling pathway activation, was stronger than that of the other control groups. The use of selective blockers showed that TLR4/NF- $\kappa$ B and ERK1/2 partly mediated oxLDL/ $\beta_2$ GPI/anti- $\beta_2$ GPI complex-induced proliferation and had an inhibitory effect on complex-stimulated apoptosis. Conversely, TLR2/p38 partly mediated oxLDL/ $\beta_2$ GPI/anti- $\beta_2$ GPI complex-induced apoptosis and had a negative effect on complex-stimulated proliferation. Specific inhibitors of NF- $\kappa$ B and ERK1/2 activation could augment the oxLDL/ $\beta_2$ GPI/anti- $\beta_2$ GPI complex-induced phosphorylation of p38 and vice versa. Under pre-treatment with NADPH oxidase inhibitors, intracellular ROS generation was confirmed to participate in oxLDL/ $\beta_2$ GPI/anti- $\beta_2$ GPI complex-induced proliferation and apoptosis, as well as the phosphorylation of NF- $\kappa$ B and MAPKs. Taken together, our data clearly revealed that the oxLDL/ $\beta_2$ GPI/anti- $\beta_2$ GPI complex had biphasic effects on VSMC survival, partly mediated by ROS-induced NF- $\kappa$ B and MAPKs activation. The TLR4/NF- $\kappa$ B and TLR2/p38 pathways played supporting roles in this dual effects-initiated signal network, and there is a trade-off relationship between the phosphorylation of NF- $\kappa$ B, ERK1/2 and p38. The dual effects of the oxLDL/ $\beta_2$ GPI/anti- $\beta_2$ GPI complex on VSMC survival contribute to the development of the structure typical of atherosclerotic lesions, particularly focal excessive growth alternating with necrosis.

### 1. Introduction

Atherosclerosis (AS) is a multifactorial and multistep disease that involves the chronic inflammatory/immune response of vascular cells at every phase of plaque formation from initiation to progression and finally to rupture. To respond to vascular injury, vascular smooth muscle cells exhibit phenotypic and functional plasticity [1]. During early atherogenesis, the aberrant proliferation of VSMC (vascular smooth muscle cell) is a hallmark of the vascular wall response to

various injuries, including mechanical and immune injury [1,2]. Increased VSMC proliferation and migration promote plaque formation in early lesions, while intriguing evidence revealed that VSMC apoptosis may be a central factor in plaque vulnerability and its subsequent sequelae [3,4]. In advanced lesions, plaque rupture occurs most commonly in the shoulder area of the plaque, a region characterized by a high rate of apoptosis of VSMC [2]. In particular, hyperplastic tissue proliferation alternating with necrosis is apparent in atherosclerotic lesions, contributing to the development of the structure typical of the

**Abbreviations:** AS, atherosclerosis; VSMC, vascular smooth muscle cell; TLR4, toll-like receptor 4; TLR2, toll-like receptor 2; oxLDL, oxidized low-density lipoprotein;  $\beta_2$ GPI,  $\beta_2$ -glycoprotein I; anti- $\beta_2$ GPI, anti- $\beta_2$ -glycoprotein I; APS, antiphospholipid syndrome; aPL, antiphospholipid antibodies; LPS, lipopolysaccharide; NF- $\kappa$ B, nuclear factor kappa B; mitogen-activated protein kinases, MAPKs; A7r5, rat thoracic aorta smooth muscle cell line; HCASMC, human coronary artery smooth muscle cells; PCNA, proliferating cell nuclear antigen; NPI, nuclear protein import; NPC, nuclear pore complex; ROS, reactive oxygen species

\* Corresponding author at: Department of Clinical Laboratory and Hematology, School of Medicine, Jiangsu University, 301 Xuefu Road, Zhenjiang, Jiangsu 212013, PR China.

E-mail address: [hongzhou@ujs.edu.cn](mailto:hongzhou@ujs.edu.cn) (H. Zhou).

<https://doi.org/10.1016/j.cellsig.2019.02.002>

Received 2 October 2018; Received in revised form 2 February 2019; Accepted 5 February 2019

Available online 07 February 2019

0898-6568/© 2019 Elsevier Inc. All rights reserved.

atherosclerotic lesion [2,5]. Such extreme changes are also the pathological basis of several severe complications of atherosclerosis, such as arterial stenosis, arterial rupture with hemorrhage and plaque rupture.

Oxidized low density lipoprotein (oxLDL) has been implicated in atherogenesis by inducing multiple functional modifications in vascular cells [6]. In vivo and in vitro studies have shown that oxLDL is capable of inducing various pro-atherogenic effects on VSMC, including proliferation, foam cell formation, migration and calcification [7–10]. Conversely, oxLDL also triggers the apoptosis of macrophages and VSMCs in the arterial wall, which accelerates the progression of fatty-streak lesions to complicated atheromatous lesions and contributes to plaque rupture [2,3,11]. Regarding these paradoxical findings, several hypotheses have been proposed to clarify the mechanism through which oxLDL can induce both VSMC proliferation and apoptosis. 1) Barbro Björkerud et al. (1996) found that the dual effects of oxLDL, i.e., strong promotion of growth or induction of cell death by apoptosis, depend on the degree of change by oxidation. These authors proved that shortly oxidized LDL had a markedly increased growth-promoting effect on VSMC, while highly oxidized LDL presented a pro-apoptosis effect [5]. 2) Max G. Bachem et al. demonstrated that a low concentration of oxLDL was profibrogenic by stimulating extracellular matrix synthesis, whereas a higher oxLDL concentration induced apoptosis in coronary artery smooth muscle cells [12]. 3) In 2009, Mirna N et al. reported that limited exposure to oxLDL may influence VSMC proliferation and apoptosis through effects on nucleocytoplasmic trafficking [13]. These authors found that short oxLDL exposure activated the ERK MAPK pathway, upregulated nuclear protein import (NPI) and nuclear pore complex (NPC) expression, and stimulated cell proliferation. In contrast, longer oxLDL exposure increased the activation of the p38 MAPK pathway, inhibited the expression of NPI and NPC, and induced the activation of genes that cause cell apoptosis. These three hypotheses suggest that the degree of oxidation, and the concentration of and exposure time to oxLDL may play crucial roles in the dual effects of oxLDL on VSMC. However, these papers have not clarified the mechanisms through which oxLDL exerts its dual effects and why oxLDL can induce these conflicting modifications on VSMC survival.

Interestingly, similar biphasic effects were also found in reactive oxygen species (ROS)-mediated phenotype changes in vascular endothelial and smooth muscle cells [14]. The ROS generated within VSMC can either induce cell growth or apoptosis through the MAPK pathway, thereby leading to vascular dysfunction. The species and amounts of ROS are likely key factors in determining the response of a cell to ROS production. Notably, oxLDL can induce the production of ROS in vascular cells mainly by a NADPH oxidase-dependent mechanism, implying a close association between the similar dual effects of oxLDL and ROS [15]. However, this interesting topic has not previously been investigated.

Antiphospholipid syndrome (APS) is characterized by the presence of antiphospholipid antibodies (aPL), including anti- $\beta_2$ -glycoprotein I antibodies (anti- $\beta_2$ GPI), anticardiolipin antibodies and lupus anticoagulants.  $\beta_2$ GPI, which can bind to oxLDL via domain V, is the major antigenic target of aPL in APS [16]. In previous studies, we proposed that the oxLDL/ $\beta_2$ GPI/anti- $\beta_2$ GPI complex, the combination of the oxLDL/ $\beta_2$ GPI complex and anti- $\beta_2$ GPI, is a circulating immune complex that could exert pro-atherogenic effects on vascular cells in atheroma plaque formation with an autoimmune background [17–19]. We have demonstrated that the oxLDL/ $\beta_2$ GPI/anti- $\beta_2$ GPI complex could further enhance the foam cell formation of macrophages and VSMCs and the expression of inflammatory cytokines via the TLR4/NF- $\kappa$ B pathway. We propose that a profound understanding of VSMC behavior in atherosclerosis induced by the oxLDL/ $\beta_2$ GPI/anti- $\beta_2$ GPI complex is critical to identify therapeutic targets to both prevent and treat atherosclerosis with an autoimmune background.

Therefore, the purposes of this study were to 1) determine how the survival of VSMC will change in response to relatively short or longer

exposure to the oxLDL/ $\beta_2$ GPI/anti- $\beta_2$ GPI complex, 2) examine specific receptors and molecules (i.e., TLR4, TLR2, NF- $\kappa$ B, and MAPKs) that may participate in the regulation of these phenotype changes and 3) investigate the possibility that the oxLDL/ $\beta_2$ GPI/anti- $\beta_2$ GPI complex modulates VSMC survival partly by the ROS-mediated activation of signaling molecules. A full understanding of how the oxLDL/ $\beta_2$ GPI/anti- $\beta_2$ GPI complex regulates mitogenesis and apoptosis in VSMC will permit the development of novel strategies to prevent or ameliorate vascular diseases in which these phenotypes predominate.

## 2. Materials and methods

### 2.1. Cell lines and cell culture

The rat thoracic aorta smooth muscle cell line (A7r5) was obtained from the Shanghai Institutes for Biological Sciences (Shanghai, China), and human coronary artery smooth muscle cells (HCASMC) were purchased from the American type culture collection (ATCC, Manassas, VA, USA). A7r5 cells and HCASMC were maintained in DMEM (Gibco BRL, Grand Island, NY, USA) supplemented with 10% FBS (Gibco BRL) at 37 °C in an incubator containing 5% CO<sub>2</sub> and routinely passaged at 90% subconfluency. Cells were stimulated with various combinations of 50  $\mu$ g/ml oxLDL (Biomedical Technologies, Inc., Stoughton, MA, USA), 100  $\mu$ g/ml  $\beta_2$ GPI (US Biological, Swampscott, MA, USA) and 100  $\mu$ g/ml anti- $\beta_2$ GPI (Chemicon, Temecula, CA, USA) for the indicated times. The oxLDL/ $\beta_2$ GPI and oxLDL/ $\beta_2$ GPI/anti- $\beta_2$ GPI complexes were prepared by incubating oxLDL with  $\beta_2$ GPI at 37 °C and pH 7.4 for 16 h as previously described [20]. 500 ng/ml LPS (Sigma) and 1  $\mu$ g/ml Pam3CSK4 (Invitrogen, San Diego, CA, USA) were used as positive control of TLR4 and TLR2 ligands respectively. The concentration of the above reagents was based on preliminary experiments and previous studies [17–20]. For some experiments, cells were pretreated with 5  $\mu$ M TLR4 inhibitor TAK-242 (Invitrogen), 10  $\mu$ M TLR2 inhibitor anti-TLR2-IgG (Invitrogen), 20  $\mu$ M NF- $\kappa$ B inhibitor PDTC (Sigma), 10  $\mu$ M p38 inhibitor SB203580 (Sigma), or 5  $\mu$ M ERK inhibitor U0126 (Promega, Madison, WI, USA) for 2 h. The absence of endotoxin containment (< 0.03 EU/ml) in all reagents (except for LPS) was guaranteed by the Limulus amoebocyte lysate assay (ACC, Falmouth, MA, USA).

### 2.2. Western blotting analysis

Total protein was extracted from the cells, and western blot analysis was performed as previously described [17–19]. Primary antibodies against  $\beta$ -actin (1:5000, Bioworld, Nanjing, Jiangsu, China), PCNA (1:500, Santa Cruz Biotechnology, Dallas, Texas, USA), Bcl-2 (1:500, Bioworld), Bax (1:1000, Cell Signaling Technology), cleaved caspase-3 (1:500, Wanleibio, Shenyang, Jilin, China), TLR4 (1:500, Santa Cruz Biotechnology), TLR2 (1:1000, Cell Signaling Technology, Beverly, MA, USA), NF- $\kappa$ B p65 (1:1000, Cell Signaling Technology), phospho-NF- $\kappa$ B-p65 ser536 (1:1000, Cell Signaling Technology), ERK1/2 (1:500, Santa Cruz Biotechnology), phospho-ERK1/2 (1:500, Santa Cruz Biotechnology), p38 (1:500, Santa Cruz Biotechnology), phospho-p38 (1:500, Santa Cruz Biotechnology), JNK (1:500, Santa Cruz Biotechnology), and phospho-JNK (1500, Santa Cruz Biotechnology) were used. Secondary antibodies were purchased from Bioworld.

### 2.3. CCK-8 assay

Cell proliferation was measured using Cell Counting Kit-8 (Dojindo, kamimashiki gun, Kumamoto, Japan). Briefly, cells ( $4 \times 10^3$  cells/well) were seeded onto 96-well plates and treated with the indicated stimuli. After incubation for 24 h, the supernatants were removed, and 100  $\mu$ l of CCK-8 working solution was added to each well for another 1.5 h at 37 °C. The CCK-8 working solution was prepared with CCK-8 stock solution and DMEM medium at a 1:10 ratio. The absorbance was measured at 450 nm with a kinetic microplate reader (Victor3 1420

Multilabel Counter; PerkinElmer, Waltham, MA, USA) to calculate the cell viability in different groups.

#### 2.4. Edu detection

The BeyoClick™ Edu cell proliferation kit with Alexa Fluor 555 (Beyotime, Shanghai, China) was used, according to the manufacturer's protocols, to measure the ability of VSMC to proliferate under different stimulations. Briefly, cells ( $4 \times 10^3$  cells/100  $\mu$ l/well) were seeded onto 96-well plates under different treatments. After incubation for 24 h, 100  $\mu$ l of 2X Edu solution (20  $\mu$ M) was added to each well to obtain a 1X Edu solution (10  $\mu$ M). Then, cells were incubated with 1X Edu solution for 2 h, and subsequently fixed with 4% paraformaldehyde for 20 min at room temperature (RT) and permeabilized with 0.3% Triton X-100 in PBS for 15 min at RT. The permeabilization buffer was then removed, and 50  $\mu$ l of 1X Click reaction solution was added to each well, followed by incubation for 30 min at RT protected from light. For nuclear staining, cells were incubated with 1X Hoechst 33342 for 10 min at RT protected from light. Between each step above, cells were washed three times with 3% BSA in PBS for 5 min at RT. Finally, cells were photographed with a fluorescence microscope (Olympus Corporation, Tokyo, Japan) at  $\times 200$  magnification. The nuclei of proliferative cells could be stained with Edu and presented in red fluorescence.

#### 2.5. Annexin V-FITC/PI apoptosis detection

The apoptosis rate of A7r5 cells was detected using an annexin V-fluorescein isothiocyanate (FITC) apoptosis-detection kit (BD Biosciences, San Jose, CA, USA) according to the manufacturer's protocols. After 48 h of stimulation, the cells were washed with PBS and resuspended in 1X binding buffer at a concentration of  $1 \times 10^6$  cells/ml and then stained with FITC annexin V and propidium iodide at RT for 15 min in the dark. Then, the cell-apoptosis (Q2 + Q3) rate was detected using flow cytometry (BD Biosciences). The data were analyzed using FlowJo software (Version 10.0.7).

#### 2.6. Real-time quantitative PCR analysis

Semiquantitative PCR analysis was used to assess the levels of TLR4 and TLR2 mRNA following the incubation of VSMC with different stimulations as previously described [17–19]. The following primer sequences were synthesized by Sangon Biotech (Shanghai, China) and used for qPCR: 5'-TCGGTGGTCAGTGTG CTTGTGG-3' and 5'-AAAGCTGAAAGCGGGGCACTCC-3' for TLR4 (amplicon size of 208 bp); 5'-TGACGAGAACAATGACGCGG-3' and 5'-GGGCCACTCCAGGTATGTCT-3' for TLR2 (amplicon size of 121 bp); 5'-CCC ATCTATGAGGGTTACGC-3' and 5'-TTTAATGTCACGCACGATTTC-3' for  $\beta$ -actin (amplicon size of 150 bp). The mRNA level of the target genes relative to the control gene  $\beta$ -actin was calculated using the  $2^{-\Delta\Delta C_t}$  method.

#### 2.7. Mitochondrial membrane potential ( $\Delta\Psi_m$ )

The fluorescent, lipophilic and cationic probe, JC-1 (Beyotime, Shanghai, China), was employed to determine the mitochondrial membrane potential (MMP) ( $\Delta\Psi_m$ ) of A7r5 cells. After 48 h of stimulation, adherent cells were washed twice with PBS, followed by incubation with JC-1 staining solution (5  $\mu$ g/ml) for 20 min at 37 °C. The cells were then washed twice with PBS, and the images were captured with a fluorescence microscope (Olympus) at  $\times 200$  magnification. JC-1 forms a red fluorescent aggregate at hyperpolarized membrane potentials, whereas it presents in the green fluorescent monomeric form at depolarized membrane potentials. The ratio of aggregate-to-monomer fluorescence was calculated by Imagepro-Plus software (version 6.0) to assess MMP, the decrease of which is a landmark change during early apoptosis.

#### 2.8. ROS detection

Intracellular ROS levels were determined by measuring the oxidative conversion of dichlorofluorescein diacetate (DCFH-DA) to the fluorescent compound dichlorofluorescein (DCF) using an ROS assay kit (Beyotime). After different stimulations, the cells were washed twice with PBS and incubated with 10  $\mu$ mol/L DCFH-DA for 20 min at 37 °C. Then, the images were captured with a fluorescence microscope (Olympus) at  $\times 200$  magnification. DCF-positive cells presented green fluorescence. In addition, the cells were collected, and DCF fluorescence intensities were analyzed using a flow cytometer, with excitation at 488 nm and emission at 525 nm. The data were analyzed using FlowJo software (version 10.0.7). The FITC-A subset is the group of DCF-positive cells.

#### 2.9. Statistical analysis

All experiments were performed in triplicate or quadruplicate and repeated at least 3 times. Data are expressed as the means  $\pm$  SDM. Statistical significance was examined using Student's unpaired *t*-test (two tailed) for two-group comparisons and one-way analysis of variance with Dunnett's posttest for multiple-group comparisons. Statistical evaluation was performed using the SPSS statistical software package (version 20.0, IBM Corp., Armonk, NY, USA). *P* < .05 indicates a statistically significant difference.

### 3. Results

#### 3.1. Biphasic and time-dependent effects of the oxLDL/ $\beta_2$ GPI/anti- $\beta_2$ GPI complex on VSMC proliferation and apoptosis

In this study, we first tested whether the oxLDL/ $\beta_2$ GPI/anti- $\beta_2$ GPI complex could alter the proliferation and apoptosis of VSMC. To obtain a comprehensive view of the survival change, HCASMC and A7r5 were stimulated with the oxLDL/ $\beta_2$ GPI/anti- $\beta_2$ GPI complex at different time gradients. Proliferating cell nuclear antigen (PCNA) protein expression, Edu staining and CCK-8 assay were used to assess cell proliferation, while western blotting for cleaved-caspase-3, Bcl-2 and Bax, as well as Annexin V-FITC/PI apoptosis detection, were used for evaluating cell apoptosis. As shown in Fig. 1A, C and E, in HCASMC, a profound increase in proliferation occurred after 6 h of stimulation and then gradually decreased. However, the apoptosis of HCASMC transiently decreased at 6 h and then significantly increased at 24 h. Furthermore, the proliferation and apoptosis of A7r5 cells treated with the oxLDL/ $\beta_2$ GPI/anti- $\beta_2$ GPI complex showed similar change at 24 and 48 h, respectively (Fig. 1B, D and F).

To further confirm the critical role of the oxLDL/ $\beta_2$ GPI/anti- $\beta_2$ GPI complex in the pathological mechanism of atheromatous plaque progression, HCASMC and A7r5 cells were incubated with different stimuli (media, oxLDL, oxLDL/ $\beta_2$ GPI, oxLDL/anti- $\beta_2$ GPI, oxLDL/ $\beta_2$ GPI/anti- $\beta_2$ GPI and  $\beta_2$ GPI/anti- $\beta_2$ GPI) for the indicated times. The results showed that the oxLDL/ $\beta_2$ GPI/anti- $\beta_2$ GPI complex could further increase PCNA and Bcl-2 protein expression, cell numbers and Edu-positive-cell percentages when compared with the effects of other control groups (Figs. 2 and 3, *P* < .05 vs. media, oxLDL, oxLDL/ $\beta_2$ GPI, oxLDL/anti- $\beta_2$ GPI and  $\beta_2$ GPI/anti- $\beta_2$ GPI) in both HCASMC and A7r5 cells. Similarly, cleaved-caspase, Bax protein expression and apoptosis percentages were upregulated in the oxLDL/ $\beta_2$ GPI/anti- $\beta_2$ GPI complex group when compared with those in the other control groups (Figs. 2 and 3, *P* < .05 vs. media, oxLDL, oxLDL/ $\beta_2$ GPI, oxLDL/anti- $\beta_2$ GPI and  $\beta_2$ GPI/anti- $\beta_2$ GPI).

#### 3.2. Stimulation of NF- $\kappa$ B and MAPK phosphorylation by the oxLDL/ $\beta_2$ GPI/anti- $\beta_2$ GPI complex in A7r5 cells and the involvement of TLRs

The NF- $\kappa$ B and MAPK pathways, involving a series of protein kinase

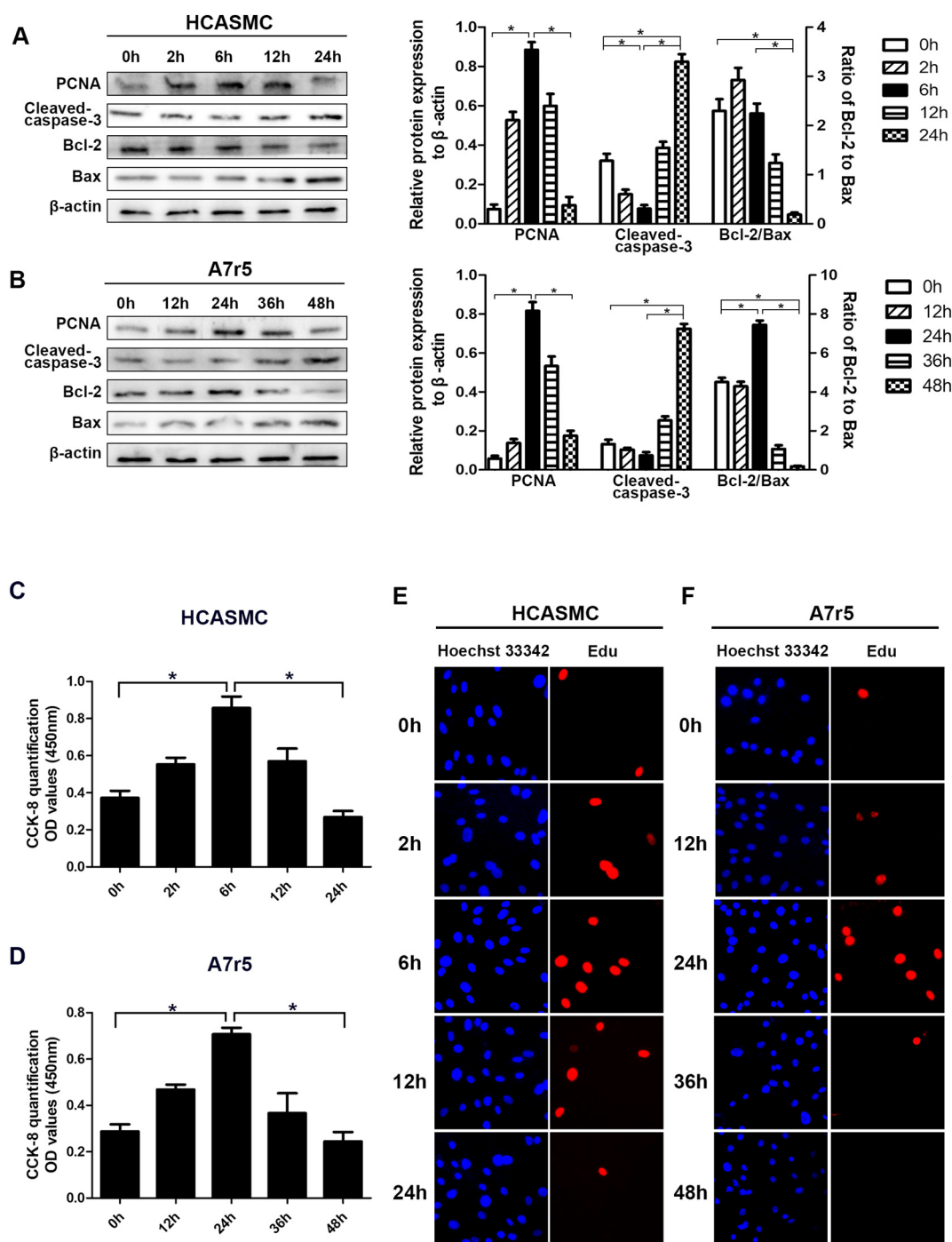


**Fig. 1.** The time-dependent effects of the oxLDL/ $\beta_2$ GPI/anti- $\beta_2$ GPI complex on VSMC proliferation and apoptosis. HCASMC and A7r5 cells were treated with the oxLDL/ $\beta_2$ GPI/anti- $\beta_2$ GPI complex for different time gradients. The expression profiles of different proliferation and apoptosis proteins were detected and quantified by western blotting (A and B). The data for PCNA and cleaved-caspase-3 were plotted on the left Y axis, and the ratio of Bcl-2 to Bax was plotted on the right Y axis. CCK-8 assay (C and D) and Edu staining (E and F) were used to detect cell proliferation ability under different times of stimulation. The data are expressed as the means  $\pm$  standard error of the mean ( $n = 3$  per group). \* $P < .05$ .

cascades, play a critical role in the regulation of mammalian cell survival. In the present study, we explored which pattern of the oxLDL/ $\beta_2$ GPI/anti- $\beta_2$ GPI complex influences the phosphorylation of NF- $\kappa$ B and MAPKs in A7r5 cells. As shown in Fig. 4 and Fig. S1, the oxLDL/ $\beta_2$ GPI/anti- $\beta_2$ GPI complex induced the phosphorylation of NF- $\kappa$ B, ERK1/2 and p38 in a time-dependent manner. It was found that the phosphorylation of NF- $\kappa$ B and ERK1/2 gradually increased after stimulation, reached a peak at 24 h and then declined quickly from 36 to 48 h. In contrast, the phosphorylation of p38 remained stable before 24 h and dramatically

increased between 24 and 48 h. However, the oxLDL/ $\beta_2$ GPI/anti- $\beta_2$ GPI complex had no effect on the phosphorylation of JNK in A7r5 cells (data not shown). Furthermore, oxLDL/ $\beta_2$ GPI/anti- $\beta_2$ GPI complex-induced NF- $\kappa$ B and MAPKs activation were all stronger than other groups at corresponding time points (Figs. 4 B,  $P \leq .05$  vs. media, oxLDL, oxLDL/ $\beta_2$ GPI, oxLDL/anti- $\beta_2$ GPI and  $\beta_2$ GPI/anti- $\beta_2$ GPI), which were consistent with our previous study [17].

TLR2 and TLR4, which are among the best studied members of the Toll-like receptor family, have been demonstrated to elicit immune

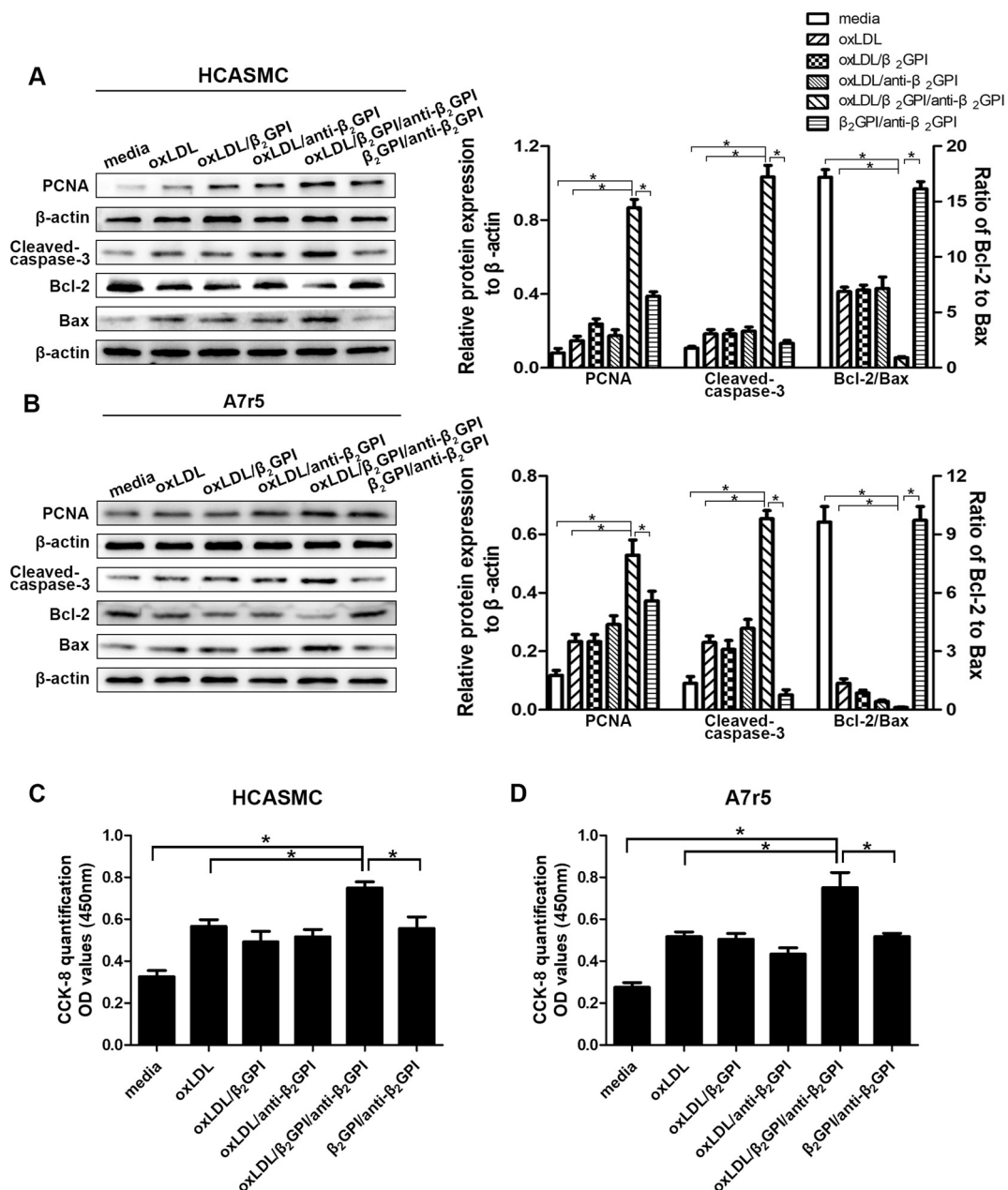


**Fig. 2.** The strongest promotion effects of the oxLDL/ $\beta_2$ GPI/anti- $\beta_2$ GPI complex on VSMC proliferation and apoptosis. HCASMC and A7r5 cells were treated with media, oxLDL, oxLDL/ $\beta_2$ GPI, oxLDL/anti- $\beta_2$ GPI, oxLDL/ $\beta_2$ GPI/anti- $\beta_2$ GPI complex and  $\beta_2$ GPI/anti- $\beta_2$ GPI for the indicated times. The expression profiles of different proliferation and apoptosis proteins were detected and quantified by western blotting (A and B). The data for PCNA and cleaved-caspase-3 were plotted on the left Y axis, and the ratio of Bcl-2 to Bax was plotted on the right Y axis. The CCK-8 assay (C and D) was used to detect cell proliferation ability under different treatments. The proliferation-related index (PCNA protein and CCK-8) was measured at 6 h for HCASMC and at 24 h for A7r5 cells. Apoptosis-related proteins (cleaved caspase-3, Bcl-2 and Bax) were measured at 24 h for HCASMC and at 48 h for A7r5. The data are expressed as the means  $\pm$  standard error of the mean ( $n = 3$  per group). \* $P < .05$ .

responses and inflammation when activated and are candidate mediators of atherogenic inflammation [21]. To reveal whether TLR2 and TLR4 were implicated in oxLDL/ $\beta_2$ GPI/anti- $\beta_2$ GPI complex-induced NF- $\kappa$ B and MAPK activation, we treated A7r5 cells with the TLR4 inhibitor TAK-242 or the TLR2 inhibitor anti-TLR2-IgG prior to stimulation with the oxLDL/ $\beta_2$ GPI/anti- $\beta_2$ GPI complex. As shown in Fig. 5A, TAK-242 partly attenuated the oxLDL/ $\beta_2$ GPI/anti- $\beta_2$ GPI complex-induced phosphorylation of NF- $\kappa$ B at 24 h of stimulation ( $P < .05$  vs. oxLDL/ $\beta_2$ GPI/anti- $\beta_2$ GPI complex group without TAK-242), matching well with our previous findings [17]. However, the upregulated phosphorylation of ERK1/2 and p38 could not be blocked by TAK-242 pretreatment. Additionally, only the phosphorylation of p38 at 48 h,

but not NF- $\kappa$ B and ERK1/2 could be largely weakened by anti-TLR2-IgG (Fig. 5B,  $P < .05$  vs. oxLDL/ $\beta_2$ GPI/anti- $\beta_2$ GPI complex group without anti-TLR2-IgG). At the same time, as classic ligand of TLR4 and TLR2 respectively, both LPS and Pam3CSK4-induced signaling molecules activation could be largely attenuated by TAK-242 and anti-TLR2-IgG, validating inhibitory efficiency of TLR4 and TLR2 specific blockers (Fig. 5A and B,  $P \leq .05$  vs. positive control group without inhibitors).

To further confirm the involvement of TLR4 and TLR2 in the activation of NF- $\kappa$ B and the MAPK signaling pathway induced by the oxLDL/ $\beta_2$ GPI/anti- $\beta_2$ GPI complex, we observed the protein and mRNA expression of TLR4 and TLR2 during stimulation. As presented in Figs. 5C and D, cells treated with the oxLDL/ $\beta_2$ GPI/anti- $\beta_2$ GPI complex

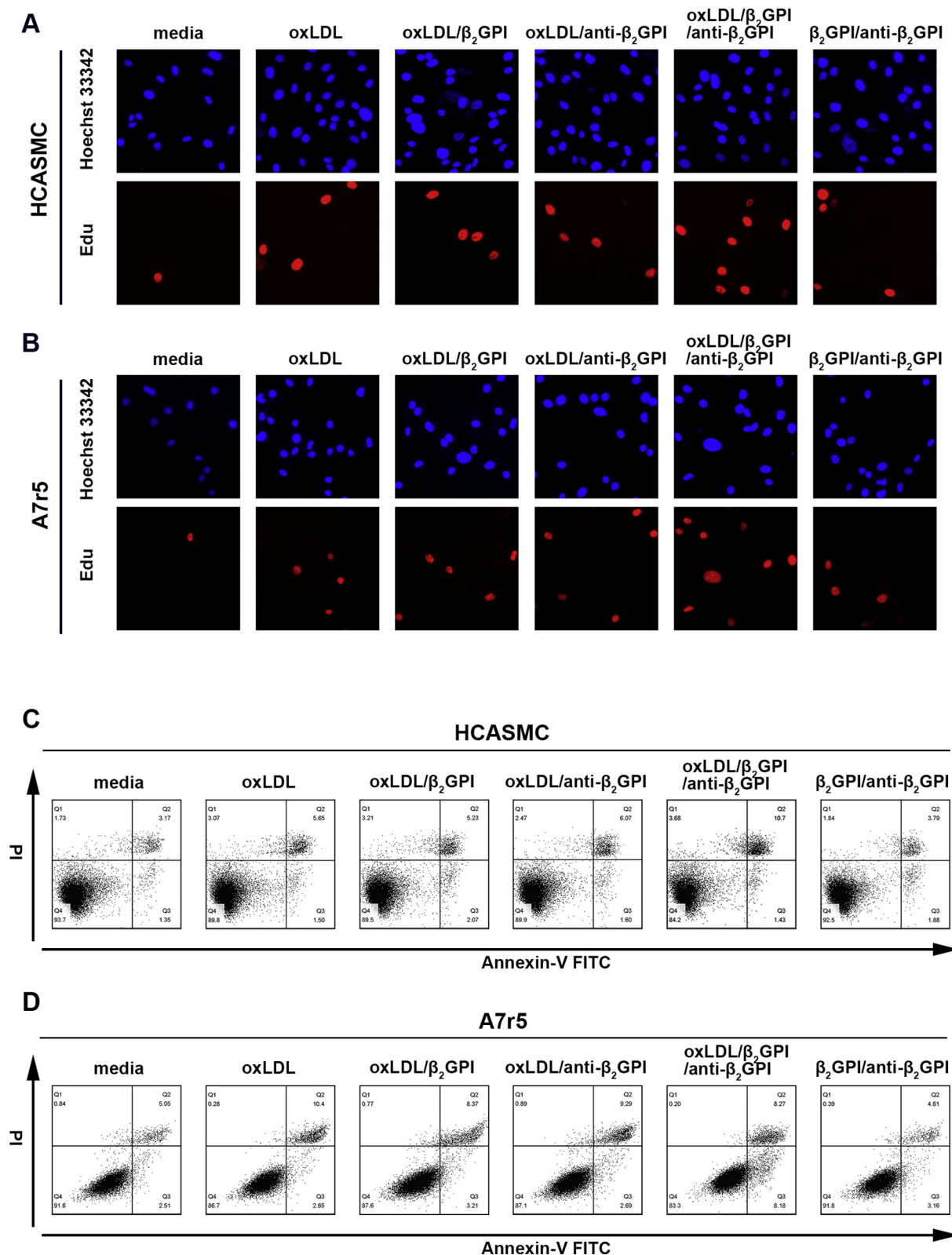


**Fig. 3.** The strongest promotion effects of the oxLDL/ $\beta_2$ GPI/anti- $\beta_2$ GPI complex on VSMC proliferation and apoptosis. HCASMC and A7r5 cells were treated with media, oxLDL, oxLDL/ $\beta_2$ GPI, oxLDL/anti- $\beta_2$ GPI, oxLDL/ $\beta_2$ GPI/anti- $\beta_2$ GPI complex and  $\beta_2$ GPI/anti- $\beta_2$ GPI for the indicated hours. Edu staining was performed after 6 h of stimulation for HCASMC (A) and at 24 h for A7r5 cells (B). Annexin-V FITC/PI apoptosis detection was performed at 24 h for HCASMC (C) and at 48 h for A7r5 cells (D).

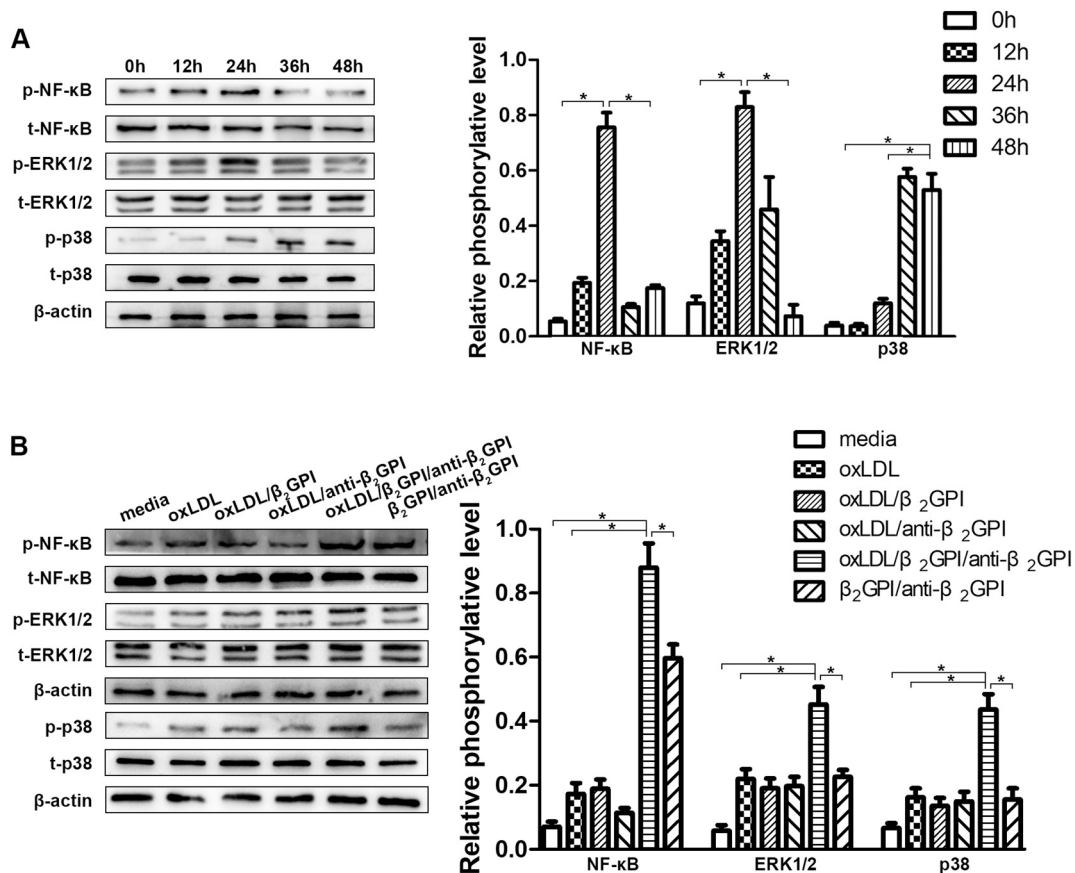


**Fig. 4.** The phosphorylation of NF-κB and MAPKs induced by the oxLDL/β<sub>2</sub>GPI/anti-β<sub>2</sub>GPI complex in A7r5 cells.

The phosphorylation of NF-κB, ERK1/2 and p38 in A7r5 cells treated with oxLDL/β<sub>2</sub>GPI/anti-β<sub>2</sub>GPI complex in a time gradient was detected and quantified by western blotting (A). Then, A7r5 cells were stimulated with media, oxLDL, oxLDL/β<sub>2</sub>GPI, oxLDL/anti-β<sub>2</sub>GPI, oxLDL/β<sub>2</sub>GPI/anti-β<sub>2</sub>GPI complex and β<sub>2</sub>GPI/anti-β<sub>2</sub>GPI for 24 or 48 h (B). The phosphorylation of NF-κB and ERK1/2 was measured at 24 h, and the phosphorylation of p38 was measured at 48 h by western blotting. The data are expressed as the means ± standard error of the mean ( $n = 3$  per group). \* $P < .05$ .

had considerably increased TLR4 expression, which has been partly proved by our previous study [17], and TLR2 expression at both the protein and mRNA levels when compared with those treated with other control groups at 24 or 48 h of stimulation ( $P < .05$  vs. media, oxLDL, oxLDL/β<sub>2</sub>GPI, oxLDL/anti-β<sub>2</sub>GPI and β<sub>2</sub>GPI/anti-β<sub>2</sub>GPI).

### 3.3. The different roles of TLRs, NF-κB, and MAPKs in oxLDL/β<sub>2</sub>GPI/anti-β<sub>2</sub>GPI complex-induced dual effects

Our study demonstrated the time-dependent dual effects of the oxLDL/β<sub>2</sub>GPI/anti-β<sub>2</sub>GPI complex on VSMC survival and the activation of TLRs, NF-κB and the MAPK signaling pathway during this process. In this study, we further investigated whether the signaling pathways explored above are involved in oxLDL/β<sub>2</sub>GPI/anti-β<sub>2</sub>GPI complex-induced VSMC survival changes. We pretreated A7r5 cells with specific inhibitors of TLR4 (TAK-242), TLR2 (anti-TLR2-IgG), NF-κB (PDTC), ERK1/2 (U0126) and p38 (SB203580) respectively. The effects of TAK-242, PDTC and U0126 are completely different from the effects of anti-TLR2-IgG and SB203580 on A7r5 cell survival. As shown in Figs. 6, 7 and Fig. S2, TAK-242, PDTC and U0126 could significantly down-regulate the complex-induced expression of proliferation proteins (PCNA) and anti-apoptosis proteins (Bcl-2), as well as the percentages of cells undergoing proliferation (Edu detection and CCK-8 assay), while apoptosis-promoting protein expression and alterations (cleaved-caspase-3, Bax and mitochondrial membrane depolarization) were largely upregulated ( $P < .05$  vs. oxLDL/β<sub>2</sub>GPI/anti-β<sub>2</sub>GPI complex group without inhibitors). In contrast, anti-TLR2-IgG and SB203580 elicited completely opposite changes in A7r5 cell survival. The results showed

that anti-TLR2-IgG and SB203580 could partly attenuate oxLDL/β<sub>2</sub>GPI/anti-β<sub>2</sub>GPI complex-stimulated mitochondrial membrane depolarization and pro-apoptosis protein expression (Figs. 6 and 7,  $P < .05$  vs. oxLDL/β<sub>2</sub>GPI/anti-β<sub>2</sub>GPI complex group without inhibitors). Additionally, PCNA and Bcl-2 expression and Edu-positive cell percentages were substantially boosted after treatment with anti-TLR2-IgG and SB203580 (Figs. 6 and 7,  $P < .05$  vs. oxLDL/β<sub>2</sub>GPI/anti-β<sub>2</sub>GPI complex group without inhibitors).

### 3.4. The trade-off relationship between the phosphorylation of NF-κB and MAPK during oxLDL/β<sub>2</sub>GPI/anti-β<sub>2</sub>GPI complex stimulation

The above studies confirmed the completely opposite roles of NF-κB, ERK1/2 and p38 in oxLDL/β<sub>2</sub>GPI/anti-β<sub>2</sub>GPI complex-induced A7r5 cell survival changes. Next, we observed the phosphorylation alterations of each signaling molecule after treatment with other molecule-specific inhibitors to further explore the signaling network underlying the implication of NF-κB, ERK1/2 and p38. As shown in Fig. 8A, treatment with PDTC could apparently increase the activation of p38 after 48 h of oxLDL/β<sub>2</sub>GPI/anti-β<sub>2</sub>GPI complex stimulation ( $P < .05$  vs. oxLDL/β<sub>2</sub>GPI/anti-β<sub>2</sub>GPI complex group without PDTC) and had no effect on ERK1/2 ( $P > .05$  vs. oxLDL/β<sub>2</sub>GPI/anti-β<sub>2</sub>GPI complex group without PDTC). Similarly, U0126 stimulation had an inducing effect on the complex-induced activation of p38 and no influence on NF-κB. In contrast, the p38 inhibitor SB203580 evidently enhanced the phosphorylation of both NF-κB and ERK1/2 after 24 h of stimulation (Fig. 8,  $P < .05$  vs. oxLDL/β<sub>2</sub>GPI/anti-β<sub>2</sub>GPI complex group without SB203580).

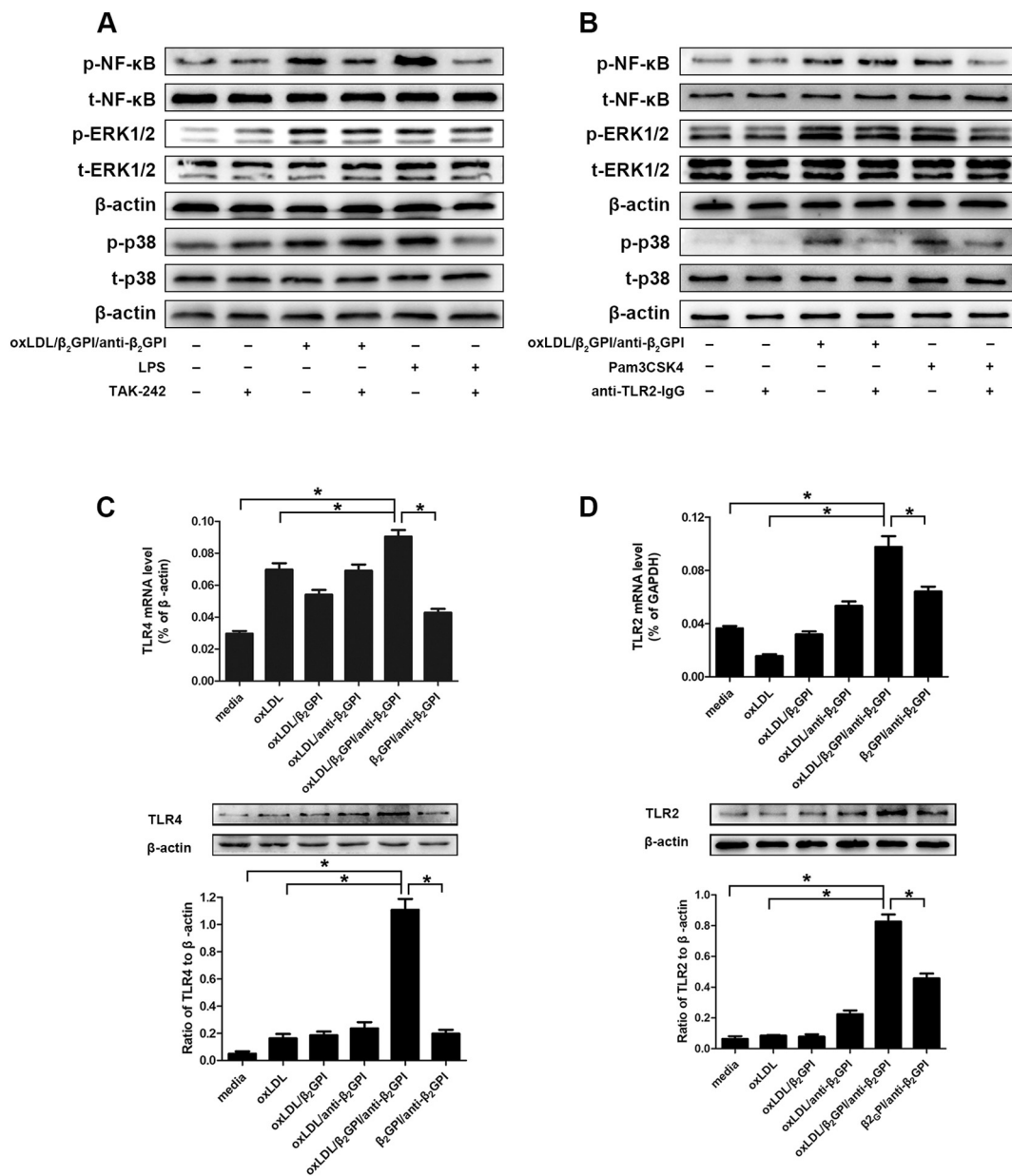


**Fig. 5.** The involvement of TLR4 and TLR2 in the phosphorylation of NF-κB, ERK1/2 and p38. A7r5 cells were pretreated with or without TAK-242 (A) or anti-TLR2-IgG (B) for 2 h, and then stimulated with oxLDL/β<sub>2</sub>GPI/anti-β<sub>2</sub>GPI complex, LPS or Pam3CSK4 for 24 or 48 h, respectively. The phosphorylation of NF-κB and ERK1/2 was measured at 24 h, and the phosphorylation of p38 was measured at 48 h by western blotting. The mRNA and protein expression of TLR4 in A7r5 cells after 24 h of different stimulations were detected by RT-qPCR and western blotting (C). The mRNA and protein expression of TLR2 in A7r5 cells after 24 h of different stimulations were measured (D). The data are expressed as the means ± standard error of the mean (n = 3 per group). \*P < .05, <sup>NS</sup>P > 0.05.

**3.5. The involvement of ROS in NF-κB and MAPK-mediated dual effects on A7r5 cell survival during oxLDL/β<sub>2</sub>GPI/anti-β<sub>2</sub>GPI complex stimulation**

Intriguing evidence has shown that excess reactive oxygen species (ROS), byproducts of aerobic metabolism, are involved in oxLDL-induced pro-atherogenic phenotype changes [22,23]. In the present study, we examined the role of ROS in the paradoxical effects of the oxLDL/β<sub>2</sub>GPI/anti-β<sub>2</sub>GPI complex on VSMC survival using two cellular ROS production inhibitors, apocynin (Apo) and diphenyleneiodonium (DPI). As shown in Fig. 9A, oxLDL/β<sub>2</sub>GPI/anti-β<sub>2</sub>GPI complex-induced ROS generation showed a subtle increase from 0 to 24 h and showed marked growth between 24 and 48 h. Also, we detected the change of Superoxide dismutase (SOD) generation. SOD activity increased apparently after stimulation and reached the peak at 24 h. Then, the

enzyme activity dropped dramatically from 24 h to 48 h (Fig. S3). We further investigated the relationship between ROS and oxLDL/β<sub>2</sub>GPI/anti-β<sub>2</sub>GPI complex-induced proliferation and apoptosis by blocking ROS generation. As shown in Fig. 9B, we first validated the inhibitory effects of Apo and DPI on ROS generation (P < .05 vs. oxLDL/β<sub>2</sub>GPI/anti-β<sub>2</sub>GPI complex group without inhibitors). Then, we pretreated A7r5 cells with Apo or DPI before stimulation with the oxLDL/β<sub>2</sub>GPI/anti-β<sub>2</sub>GPI complex. As shown in Figs. 9C and 10A, B and C, both Apo and DPI could partly decrease PCNA expression, Edu-positive cell percentage and cell counting after 24 h of oxLDL/β<sub>2</sub>GPI/anti-β<sub>2</sub>GPI complex stimulation (P < .05 vs. oxLDL/β<sub>2</sub>GPI/anti-β<sub>2</sub>GPI complex group without inhibitors). Moreover, the oxLDL/β<sub>2</sub>GPI/anti-β<sub>2</sub>GPI complex-induced apoptosis at 48 h was also blocked by treatment with Apo and DPI.

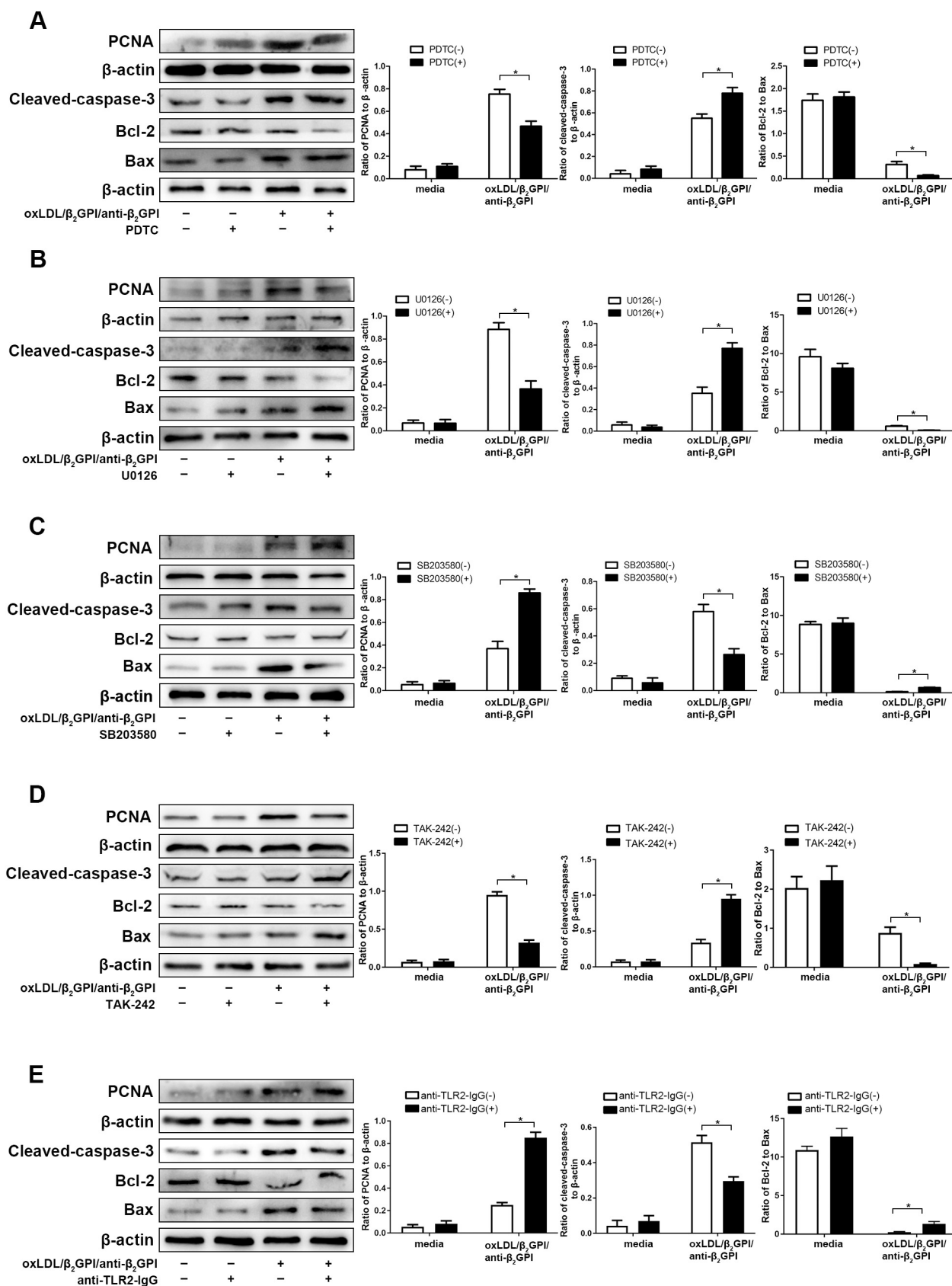
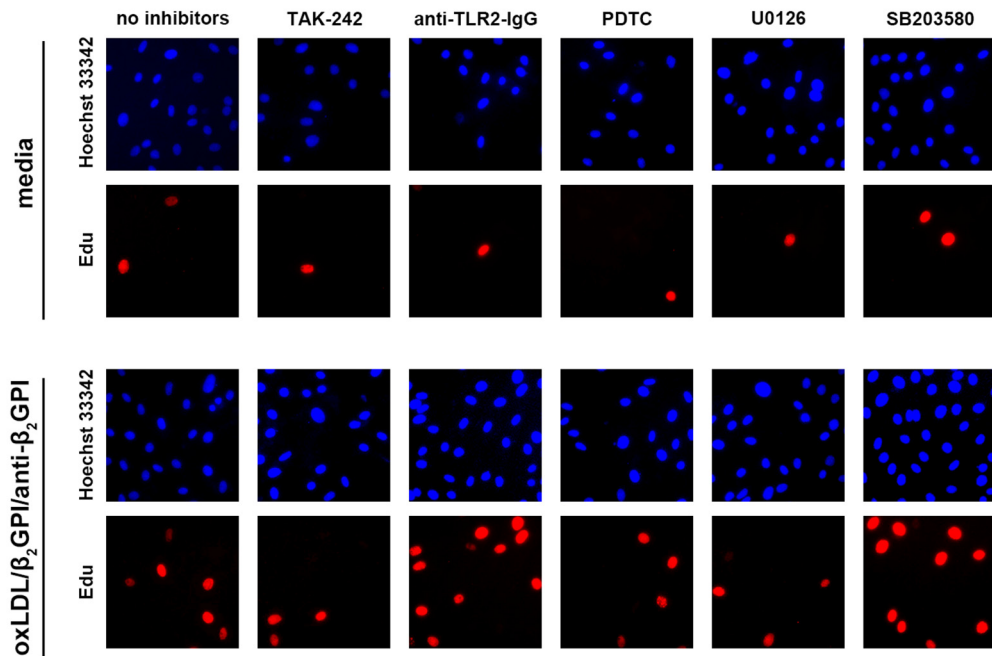
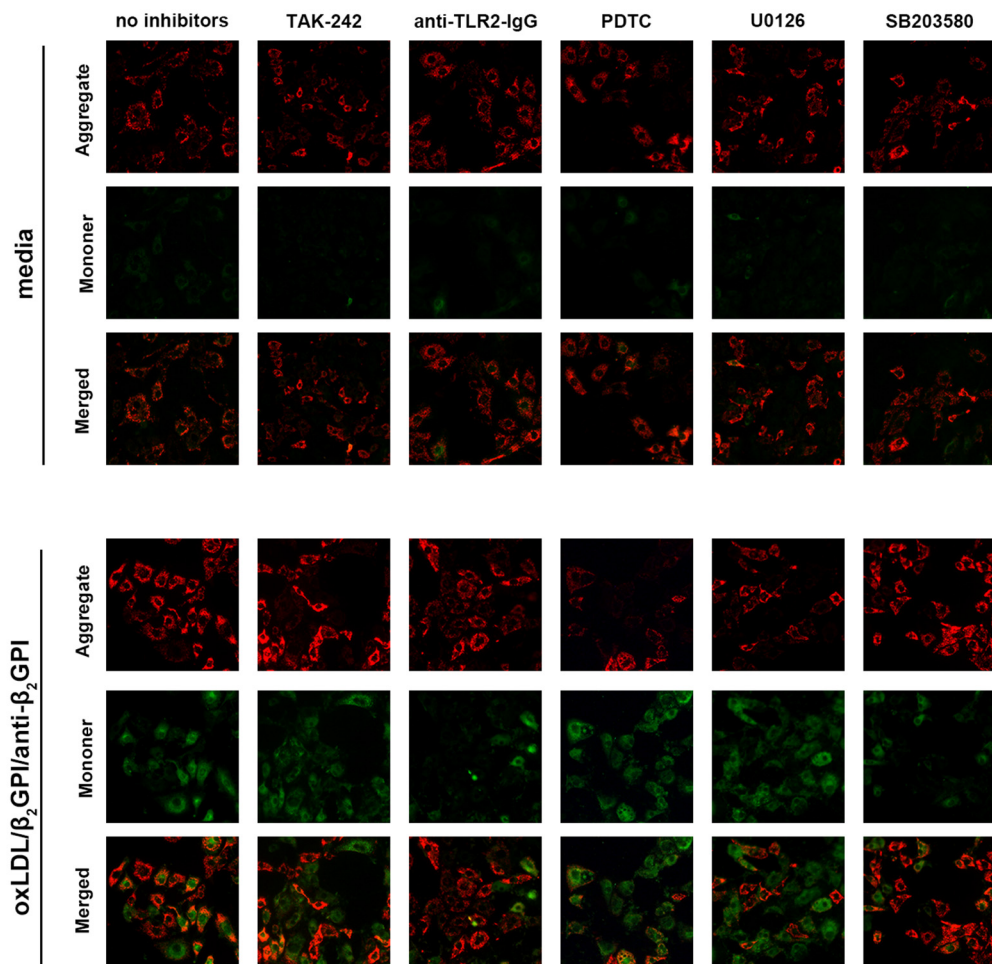


**Fig. 6.** The involvement of TLRs, NF-κB, and MAPKs in oxLDL/β<sub>2</sub>GPI/anti-β<sub>2</sub>GPI complex-induced proliferation and apoptosis in A7r5 cells. A7r5 cells were pretreated with or without PDTC, U0126, SB203580, TAK-242 or anti-TLR2-IgG for 2 h and then stimulated with the oxLDL/β<sub>2</sub>GPI/anti-β<sub>2</sub>GPI complex for 24 or 48 h. PCNA expression was detected by western blotting at 24 h and cleaved-caspase-3, Bcl-2 and Bax expression were measured after 48 h of stimulation. The data are expressed as the means ± standard error of the mean (n = 3 per group). \*P < .05.

**A**



**B**



(caption on next page)

**Fig. 7.** Different effects of TLRs, NF-κB, and MAPK inhibitors on oxLDL/β<sub>2</sub>GPI/anti-β<sub>2</sub>GPI complex-induced proliferation and apoptosis in A7r5 cells. A7r5 cells were pretreated with or without PDTC, U0126, SB203580, TAK-242 or anti-TLR2-IgG for 2 h and then stimulated with the oxLDL/β<sub>2</sub>GPI/anti-β<sub>2</sub>GPI complex for 24 or 48 h, respectively. Edu staining was performed at 24 h, and a mitochondrial membrane potential assay was performed after 48 h of stimulation. The data are expressed as the means ± standard error of the mean (n = 3 per group).

It is reported that ROS-mediated NF-κB and MAPKs act as intracellular signaling molecules in modulating phenotype changes, such as growth, apoptosis, and survival, in vascular cells [24]. Based on the above studies, we conclude that the oxLDL/β<sub>2</sub>GPI/anti-β<sub>2</sub>GPI complex likely induces opposing effects on VSMC proliferation and apoptosis by the selective activation of NF-κB and MAPKs. Hence, we further explored whether ROS were involved in the oxLDL/β<sub>2</sub>GPI/anti-β<sub>2</sub>GPI complex-induced phosphorylation of NF-κB and MAPKs to reveal the detailed molecular mechanism behind these interesting findings. As shown in Fig. 10 D, Apo and DPI could significantly inhibit the phosphorylation of NF-κB and ERK1/2 after 24 h of stimulation and the phosphorylation of p38 at 48 h, respectively (P < .05 vs. oxLDL/β<sub>2</sub>GPI/anti-β<sub>2</sub>GPI complex group without inhibitors).

**4. Discussion**

The role of autoimmunity in the pathogenic mechanism of atherosclerotic plaque formation is an important topic of investigation [25]. Accumulating reports have, to some degree, demonstrated the hypothesis that the oxLDL/β<sub>2</sub>GPI/anti-β<sub>2</sub>GPI complex is an immune complex that functions as a proatherogenic agent in AS with APS background [17–19,26–28]. Because excessive intimal growth alternating with focal massive cell apoptosis is a structure typical of atherosclerotic lesions, we propose whether these extreme alterations in plaques could be attributed to the biphasic effects of oxLDL on cell survival. In this study, we investigated whether the oxLDL/β<sub>2</sub>GPI/anti-β<sub>2</sub>GPI complex has similar dual effects on VSMC survival and explored the underlying molecular mechanism.

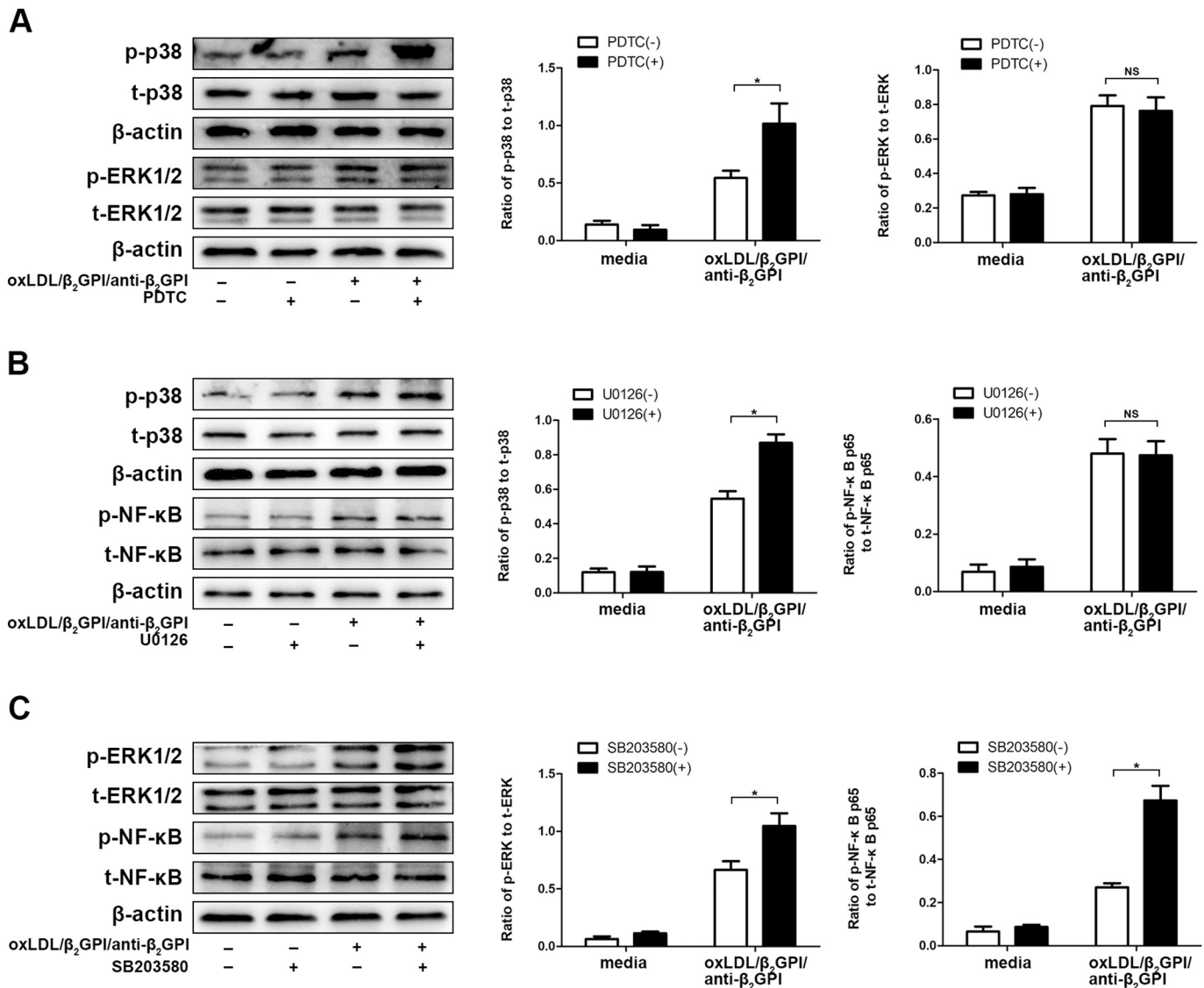
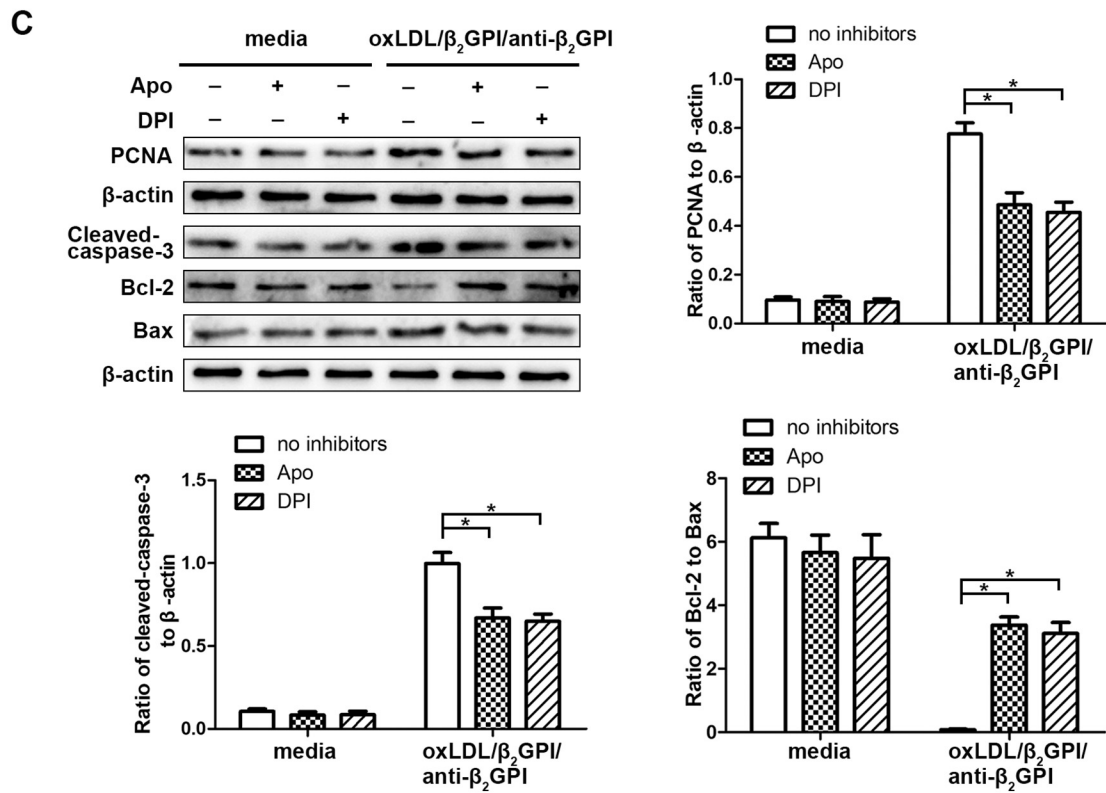
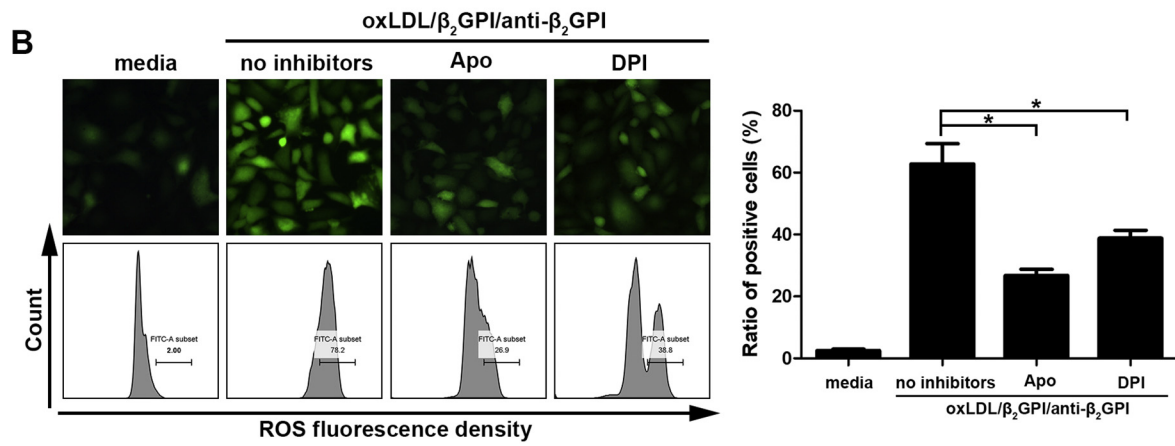
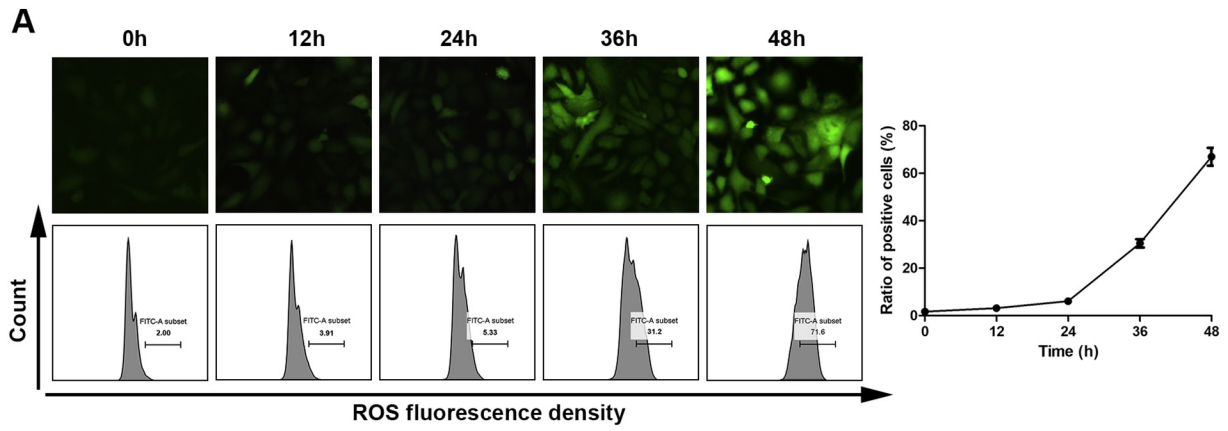


**Fig. 8.** The interaction between NF-κB, ERK1/2 and p38 activation in A7r5 cells during oxLDL/β<sub>2</sub>GPI/anti-β<sub>2</sub>GPI complex stimulation. A7r5 cells were pretreated with or without PDTC, U0126 or SB203580 for 2 h and then stimulated with the oxLDL/β<sub>2</sub>GPI/anti-β<sub>2</sub>GPI complex for 24 or 48 h. The phosphorylation of NF-κB and ERK1/2 was measured at 24 h, and the phosphorylation of p38 was measured at 48 h by western blotting. The data are expressed as the means ± standard error of the mean (n = 3 per group). \*P < .05, <sup>NS</sup>P > 0.05.



(caption on next page)

**Fig. 9.** ROS generation during oxLDL/ $\beta_2$ GPI/anti- $\beta_2$ GPI complex stimulation and its involvement in proliferation and apoptosis.

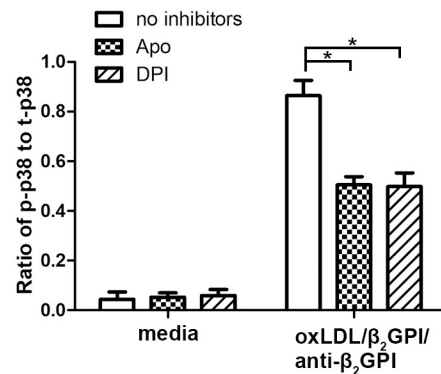
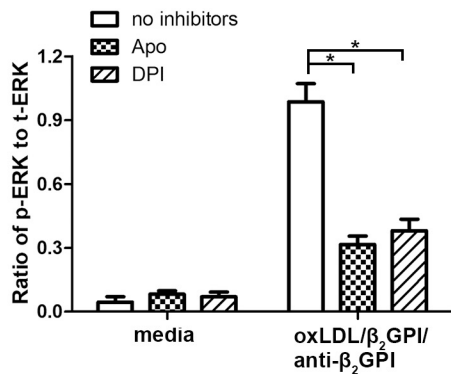
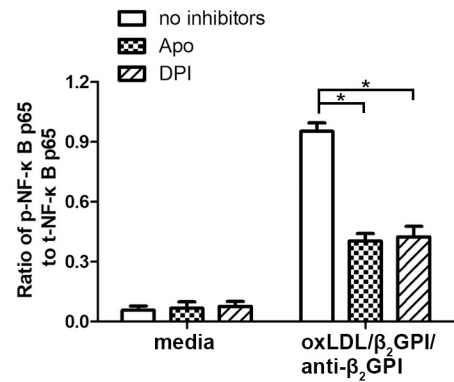
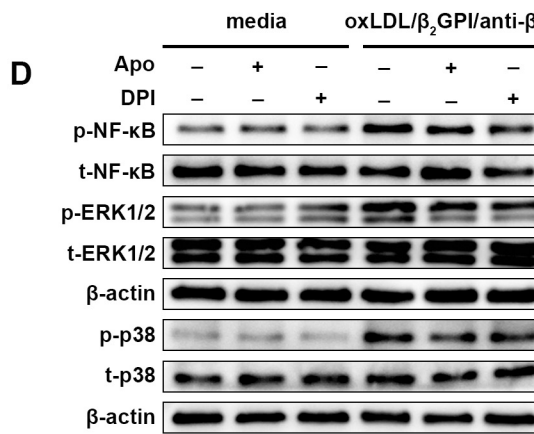
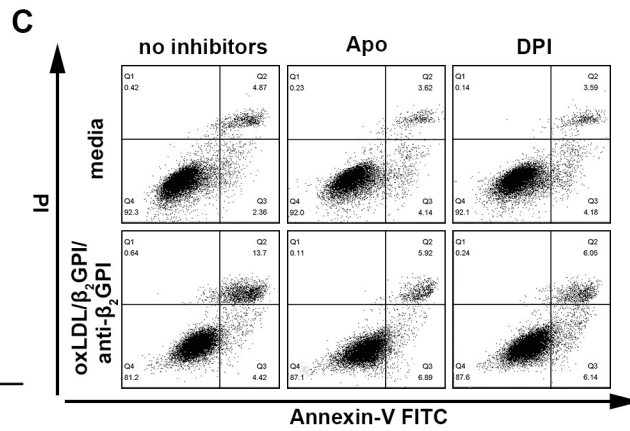
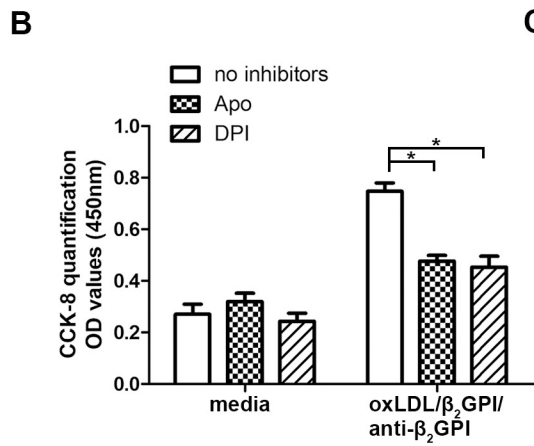
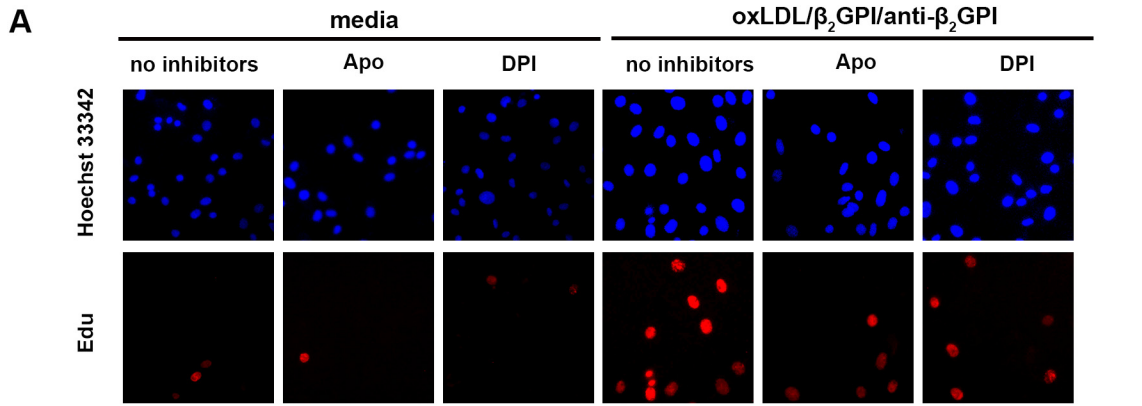
A7r5 cells were incubated with the oxLDL/ $\beta_2$ GPI/anti- $\beta_2$ GPI complex for different times, and ROS generation was detected and quantified (A). Then, A7r5 cells were pretreated with or without Apo and DPI before stimulation with the oxLDL/ $\beta_2$ GPI/anti- $\beta_2$ GPI complex for 24 or 48 h. ROS generation and apoptosis-related protein (cleaved caspase-3, Bcl-2 and Bax) were detected and quantified at 48 h (B and C). PCNA expression was detected at 24 h by western blotting (C). The data are expressed as the means  $\pm$  standard error of the mean ( $n = 3$  per group). \* $P < .05$ .

In the present study, our data showed that the short exposure of VSMC to the oxLDL/ $\beta_2$ GPI/anti- $\beta_2$ GPI complex could increase cell proliferation and mitogenic activity. Meanwhile, when VSMCs were incubated with the oxLDL/ $\beta_2$ GPI/anti- $\beta_2$ GPI complex for a longer period, the proliferative markers were diminished, and the expression of apoptosis markers was significantly enhanced. These time-dependent dual effects of the oxLDL/ $\beta_2$ GPI/anti- $\beta_2$ GPI complex on VSMC survival are consistent with the findings for oxLDL [13]. Moreover, we demonstrated that the promotion effects of the oxLDL/ $\beta_2$ GPI/anti- $\beta_2$ GPI complex on both proliferation and apoptosis were substantially stronger than those of sole oxLDL and other control groups, suggesting the absolutely important role of the oxLDL/ $\beta_2$ GPI/anti- $\beta_2$ GPI complex in the progression of AS with an autoimmune background. Interestingly, the results showed that  $\beta_2$ GPI/anti- $\beta_2$ GPI had an effect on proliferation but not on apoptosis, implying an indispensable role for oxLDL in oxLDL/ $\beta_2$ GPI/anti- $\beta_2$ GPI complex-induced apoptosis. The results also suggested that it is oxLDL that determines the capability of the oxLDL/ $\beta_2$ GPI/anti- $\beta_2$ GPI complex to exert opposing effects on proliferation and apoptosis.

The phosphorylation of cellular proteins by kinases plays a significant role in modulating cell migration, differentiation, proliferation and apoptosis in response to extracellular stimuli [24]. NF- $\kappa$ B and the MAPK family participate in the regulation of cell cycle in mammalian cells [24,29,30]. In addition, growing interest has developed in the implication of TLRs in the deterioration of AS [8,31]. Consequently, we demonstrated the involvement of TLRs, NF- $\kappa$ B and MAPKs in the biphasic effects shown in this study, as well as the cross-interaction between these proteins, in four different ways. First, oxLDL/ $\beta_2$ GPI/anti- $\beta_2$ GPI complex could induce the phosphorylation of NF- $\kappa$ B, ERK1/2 and p38 in a time-dependent manner, which is consistent with its effects on proliferation and apoptosis. These results suggest that the phosphorylation of NF- $\kappa$ B and ERK1/2 is closely correlated with oxLDL/ $\beta_2$ GPI/anti- $\beta_2$ GPI complex-induced proliferation, while the phosphorylation of p38 is potentially involved in apoptosis. In addition, the phosphorylation of NF- $\kappa$ B, ERK1/2 and p38 in the oxLDL/ $\beta_2$ GPI/anti- $\beta_2$ GPI complex group is the strongest, implying the potent pathogenic role of this complex. Second, as the main upstream inflammatory receptors of NF- $\kappa$ B and MAPKs, involvement of TLR4 and TLR2 was also examined by detecting the expression of these two proteins. Using specific blockers, the TLR4/NF- $\kappa$ B and TLR2/p38 pathways were confirmed to be activated during oxLDL/ $\beta_2$ GPI/anti- $\beta_2$ GPI complex stimulation. Third, different roles for TLRs, NF- $\kappa$ B and ERK1/2 during the oxLDL/ $\beta_2$ GPI/anti- $\beta_2$ GPI complex stimulation were also demonstrated using selective blockers. The inhibition of TLR4, NF- $\kappa$ B and ERK1/2 not only down-regulated oxLDL/ $\beta_2$ GPI/anti- $\beta_2$ GPI complex-induced proliferation in A7r5 cells but also moderately increased complex-stimulated apoptosis. Conversely, blocking TLR2 and p38 had contrasting effects on cell survival. In a word, the TLR4/NF- $\kappa$ B signaling pathway and ERK1/2 can transduce proliferation signals elicited by the oxLDL/ $\beta_2$ GPI/anti- $\beta_2$ GPI complex and negatively modulate apoptosis. However, the TLR2/p38 signaling pathway can relay the apoptosis signal induced by the oxLDL/ $\beta_2$ GPI/anti- $\beta_2$ GPI complex and have a negative effect on proliferation. Such differential activation of NF- $\kappa$ B, ERK1/2 and p38 allows VSMC induced by the oxLDL/ $\beta_2$ GPI/anti- $\beta_2$ GPI complex to use the same second messenger to elicit varied responses. Part of the effects observed here are consistent with the findings for oxLDL [13]. However, these authors did not move forward to discuss the cross-interaction between signaling molecule-mediated proliferation and apoptosis. Fourth, based on the above findings, in this study, we examined our hypothesis that

the negative regulation of NF- $\kappa$ B and ERK1/2 activation on apoptosis, as well as the negative effect of p38 on proliferation, can be attributed to the changes in the phosphorylation of corresponding signaling molecules. Hence, we observed the interactions between the phosphorylation of NF- $\kappa$ B, ERK1/2 and p38 using selective inhibitors. As expected, the inhibition of NF- $\kappa$ B and ERK1/2 could further provoke oxLDL/ $\beta_2$ GPI/anti- $\beta_2$ GPI complex-induced p38 phosphorylation when the phosphorylation of NF- $\kappa$ B and ERK1/2 were also further enhanced by the p38 inhibitor. In summary, signaling network is extremely important for our understanding of VSMC proliferation and apoptosis under oxLDL/ $\beta_2$ GPI/anti- $\beta_2$ GPI complex stimulation. The NF- $\kappa$ B and MAPK pathways are tightly cross-communicated and mutually restrained in oxLDL/ $\beta_2$ GPI/anti- $\beta_2$ GPI complex-induced dual effects on VSMC survival. The interaction between NF- $\kappa$ B and members of the MAP kinase family involves components in common pathways, as well as positive and negative feedback signals, consequently contributing to the fate of a cell to divide or terminally differentiate. It is worth mentioning that the opposing effects of the oxLDL/ $\beta_2$ GPI/anti- $\beta_2$ GPI complex on cell growth and MAPK activity agree very well with the findings of Tombes et al. [32]. These authors proposed that the “MAP kinases cascade can either stimulate or inhibit DNA synthesis in primary cultures of rat hepatocytes depending upon whether its activation is acute/phasic or chronic”.

We further explored the role of oxidative stress in oxLDL/ $\beta_2$ GPI/anti- $\beta_2$ GPI complex-induced dual effects on VSMC survival to obtain a full understanding of the underlying mechanism. OxLDL-derived oxidative stress is characterized by excess ROS generation, most of which is dependent on NADPH oxidase activity [33]. ROS are generated by oxygen metabolism which is balanced by the rate of oxidant formation and elimination. Oxidative stress is a result of imbalance between the generation of ROS and the antioxidant defense systems. ROS can also act as intracellular signaling molecules in mediating phenotypes that may be considered both physiological and pathophysiological in VSMC [14]. In addition, ROS generated within VSMC can either induce cell mitogens or promote death, thereby leading to vascular dysfunction [14]. Hence, in this study, we investigated the association between ROS- and oxLDL/ $\beta_2$ GPI/anti- $\beta_2$ GPI complex-induced biphasic effects on VSMC survival. We also detected alteration of SOD which is an enzyme that alternately catalyzes the dismutation of the superoxide ( $O_2^-$ ) radical and is an important antioxidant defense in nearly all living cells exposed to oxidative stress. The data showed totally different time-dependent correlations of ROS generation and SOD activity, providing more supporting evidence to our hypothesis that oxidative stress which can be attributed to the imbalance in the oxidant/anti-oxidant mechanisms plays a crucial role in oxLDL/ $\beta_2$ GPI/anti- $\beta_2$ GPI complex-induced biphasic effects on VSMCs survival. Moreover, the involvement of ROS in oxLDL/ $\beta_2$ GPI/anti- $\beta_2$ GPI complex-induced proliferation and apoptosis was confirmed by inhibitors of NADPH oxidase, which could apparently attenuate ROS generation. Both oxLDL/ $\beta_2$ GPI/anti- $\beta_2$ GPI complex-induced proliferation and apoptosis were suppressed by blockers of ROS generation. In addition, oxLDL/ $\beta_2$ GPI/anti- $\beta_2$ GPI complex-induced phosphorylation of NF- $\kappa$ B and ERK1/2, as well as the phosphorylation of p38, could also be partly blunted by these inhibitors. Thus, the amount of ROS, which is closely related to the time of stimulation, is likely a key factor in determining the response of a cell to ROS production by the differential activation of transcription factors (i.e., NF- $\kappa$ B, ERK1/2 and p38). These findings were consistent with those of a previous study in which NF- $\kappa$ B and ERK1/2, as potential targets of ROS in VSMC, were implicated in VSMC proliferation and p38



(caption on next page)

**Fig. 10.** Involvement of ROS in oxLDL/ $\beta_2$ GPI/anti- $\beta_2$ GPI complex-induced proliferation and apoptosis, as well as the phosphorylation of NF- $\kappa$ B and MAPKs, in A7r5 cells.

A7r5 cells were pretreated with or without Apo and DPI prior to stimulation with the oxLDL/ $\beta_2$ GPI/anti- $\beta_2$ GPI complex for 24 or 48 h. Edu staining (A) and the CCK-8 assay (B) were performed after 24 h of stimulation, and Annexin V-FITC/PI detection (C) was performed at 48 h after stimulation. The phosphorylation of NF- $\kappa$ B and ERK1/2 was measured at 24 h, and the phosphorylation of p38 was measured at 48 h by western blotting. The data are expressed as the means  $\pm$  standard error of the mean ( $n = 3$  per group). \* $P < .05$ .

was involved in stress-induced apoptosis [14]. The relation between ROS generation and TLRs were also explored. Results showed that TLRs inhibitor had no significantly effects on ROS generation (Fig. S4,  $P \geq .05$  vs. oxLDL/ $\beta_2$ GPI/anti- $\beta_2$ GPI complex group without inhibitors). Based on these observations, we concluded that TLRs are not upstream receptors of ROS generation and the effects of TLR inhibitors on downstream signaling molecules activation, as well as the cell growth alteration, are not attributed to their effects on ROS generation.

In conclusion, this study combined with previous studies suggests a multilevel mechanism through which the oxLDL/ $\beta_2$ GPI/anti- $\beta_2$ GPI complex can alter VSMC proliferation and apoptosis [5,12,13] (Fig. S4). The incubation time, oxidation degree and concentration of the oxLDL/ $\beta_2$ GPI/anti- $\beta_2$ GPI complex determine the intracellular amount of ROS generation. Exposure of VSMC to relatively low levels of oxidative stress for short periods increases the phosphorylation of NF- $\kappa$ B and ERK1/2 and promotes growth, whereas prolonged exposure to higher concentrations induces the phosphorylation of p38 and leads to cell apoptosis. The NF- $\kappa$ B and MAP kinases signal transduction pathways that play an important role in the regulation of VSMC growth in a manner inextricable from other signal transduction systems potentially by sharing substrate and cross-cascade interactions. Both the TLR4/NF- $\kappa$ B and TLR2/p38 pathways act as a bypass in this signaling network to jointly contribute to the biphasic effects of the oxLDL/ $\beta_2$ GPI/anti- $\beta_2$ GPI complex on VSMC survival. The NF- $\kappa$ B and MAPK pathways integrate a wide variety of extracellular signals involved in the regulation of cell growth (Fig. S4). Cross-talk can occur at many levels from the membrane to the nucleus. The net balance between proliferation and apoptosis, which is influenced by the interaction of different signaling pathways, determines the extent of VSMC growth and the progression of the atheromatous plaque.

This study reveals the molecular mechanism underlying the biphasic effects on VSMC survival induced by the oxLDL/ $\beta_2$ GPI/anti- $\beta_2$ GPI complex. Such efforts will likely provide potential molecular targets for therapeutic intervention and novel ideas for the design of pharmacotherapeutic approaches in the field of AS with an autoimmune background through the fine modulation of oxLDL/ $\beta_2$ GPI/anti- $\beta_2$ GPI complex-regulated signaling.

## Acknowledgments

This work was supported by the National Natural Science Foundation of China (No. 81370614) to Hong Zhou, Youth Fund of Jiangsu Province (BK20150532) and Project of Natural Science in Colleges and Universities of Jiangsu Province (15KJB310002) to Ting Wang.

## Conflict of interest

Authors declare no financial or commercial conflicts of interest.

## Appendix A. Supplementary data

Supplementary data to this article can be found online at <https://doi.org/10.1016/j.cellsig.2019.02.002>.

## References

[1] G. Tellides, J.S. Pober, Inflammatory and immune responses in the arterial media, *Circ. Res.* 116 (2) (2015) 312–322.

- [2] M.R. Bennett, S. Sinha, G.K. Owens, Vascular smooth muscle cells in atherosclerosis, *Circ. Res.* 118 (4) (2016) 692–702.
- [3] Y. Akishima, Y. Akasaka, Y. Ishikawa, Z. Lijun, H. Kiguchi, K. Ito, H. Itabe, T. Ishii, Role of macrophage and smooth muscle cell apoptosis in association with oxidized low-density lipoprotein in the atherosclerotic development, *Modern Pathol. Offic. J. United States Can. Acad. Pathol. Inc* 18 (3) (2005) 365–373.
- [4] A. Frisantiene, M. Philippova, P. Erne, T.J. Resink, Smooth muscle cell-driven vascular diseases and molecular mechanisms of VSMC plasticity, *Cell. Signal.* 52 (2018) 48–64.
- [5] B. Bjorkerud, S. Bjorkerud, Contrary effects of lightly and strongly oxidized LDL with potent promotion of growth versus apoptosis on arterial smooth muscle cells, macrophages, and fibroblasts, *Arterioscler. Thromb. Vasc. Biol.* 16 (3) (1996) 416–424.
- [6] G. Maiolino, G. Rossitto, P. Caielli, V. Bisogni, G.P. Rossi, L.A. Calò, The role of oxidized low-density lipoproteins in atherosclerosis: the myths and the facts, *Mediat. Inflamm.* 2013 (2013) (2013) 714653.
- [7] J.H. Lin, S.S. Zhou, T.T. Zhao, T. Ju, L.M. Zhang, TRPM7 channel regulates ox-LDL-induced proliferation and migration of vascular smooth muscle cells via MEK-ERK pathways, *FEBS Lett.* 590 (4) (2016) 520–532.
- [8] Y.W. Yin, S.Q. Liao, M.J. Zhang, Y. Liu, B.H. Li, Y. Zhou, L. Chen, C.Y. Gao, J.C. Li, L.L. Zhang, TLR4-mediated inflammation promotes foam cell formation of vascular smooth muscle cell by upregulating ACAT1 expression, *Cell Death Dis.* 26 (6) (2014) e1574.
- [9] L.Z. Liao, Q. Zhou, Y. Song, W.K. Wu, H.M. Yu, S. Wang, Y.L. Chen, M.H. Ye, L.H. Lu, Ceramide mediates Ox-LDL-induced human vascular smooth muscle cell calcification via p38 mitogen-activated protein kinase signaling, *PLoS One* 8 (12) (2013) e82379.
- [10] J. Liu, Y.G. Ren, K. Li, L.H. Zhang, Oxidized low-density lipoprotein increases the proliferation and migration of human coronary artery smooth muscle cells through the upregulation of osteopontin, *Int. J. Mol. Med.* 33 (5) (2014) 1341–1347.
- [11] J.S. Hwang, S.Y. Eun, S.A. Ham, T. Yoo, W.J. Lee, K.S. Paek, J.T. Do, D.-S. Lim, H.G. Seo, PPAR $\delta$  modulates oxLDL-induced apoptosis of vascular smooth muscle cells through a TGF- $\beta$ /FAK signaling axis, *Int. J. Biochem. Cell Biol.* 62 (2015) 54–61.
- [12] M.G. Bachem, D. Wendelin, W. Schneiderhan, C. Haug, U. Zorn, H.J. Gross, A. Schmid-Kotsas, A. Grünert, Depending on thier concentration oxidized low density lipoproteins stimulate extracellular matrix synthesis or induce apoptosis in human coronary artery smooth muscle cells, *Clin. Chem. Lab. Med. CCLM/FESCC* 37 (3) (1999) 319–326.
- [13] M.N. Chahine, D.P. Blackwood, E. Dibrov, M.N. Richard, G.N. Pierce, Oxidized LDL affects smooth muscle cell growth through MAPK-mediated actions on nuclear protein import, *J. Mol. Cell. Cardiol.* 46 (3) (2009) 431–441.
- [14] K. Irani, Oxidant signaling in vascular cell growth, death, and survival, *Circ. Res.* 87 (3) (2000) 179–183.
- [15] K. Bedard, K.H. Krause, The NOX family of ROS-generating NADPH oxidases: physiology and pathophysiology, *Physiol. Rev.* 87 (1) (2007) 245–313.
- [16] J.D. Li, Y. Chi, S.Q. Liu, L. Wang, R.J. Wang, X.F. Han, E. Matsuura, Q.P. Liu, Recombinant domain V of beta2-glycoprotein I inhibits the formation of atherogenic oxLDL/beta2-glycoprotein I complexes, *J. Clin. Immunol.* 34 (6) (2014) 669–676.
- [17] T. Wang, H. OuYang, H. Zhou, L.F. Xia, X.Y. Wang, T. Wang, Proatherogenic activation of A7r5 cells induced by the oxLDL/beta2GPI/antibeta2GPI complex, *Int. J. Mol. Med.* 42 (4) (2018) 1955–1966.
- [18] Y. Xu, X.M. Kong, H. Zhou, X.L. Zhang, J.J. Liu, J.C. Yan, H.X. Xie, Y.C. Xie, oxLDL/beta2GPI/anti-beta2GPI complex induced macrophage differentiation to foam cell involving TLR4/NF- $\kappa$ B signal transduction pathway, *Thromb. Res.* 134 (2) (2014) 384–392.
- [19] X.L. Zhang, Y.C. Xie, H. Zhou, Y. Xu, J.J. Liu, H.X. Xie, J.C. Yan, Involvement of TLR4 in oxidized LDL/beta2GPI/anti-beta2GPI-induced transformation of macrophages to foam cells, *J. Atheroscler. Thromb.* 21 (11) (2014) 1140–1151.
- [20] K. Kobayashi, M. Kishi, T. Atsumi, M.L. Bertolaccini, H. Makino, N. Sakairi, I. Yamamoto, T. Yasuda, M.A. Khamashta, G.R.V. Hughes, T. Koike, D.R. Voelker, E. Matsuura, Circulating oxidized LDL forms complexes with  $\beta_2$ -glycoprotein I, *J. Lipid Res.* 44 (4) (2003) 716–726.
- [21] P.N. Hopkins, Molecular biology of atherosclerosis, *Physiol. Rev.* 93 (3) (2013) 1317–1542.
- [22] S. Balzan, V. Lubrano, LOX-1 receptor: a potential link in atherosclerosis and cancer, *Life Sci.* 198 (2018) 79–86.
- [23] Z. Ding, S. Liu, X. Wang, M. Khaidakov, Y. Dai, J.L. Mehta, Oxidant stress in mitochondrial DNA damage, autophagy and inflammation in atherosclerosis, *Sci. Rep.* 3 (2013) 1077.
- [24] W. Zhang, H.T. Liu, MAPK signal pathways in the regulation of cell proliferation in mammalian cells, *Cell Res.* 12 (1) (2002) 9–18.
- [25] E. Matsuura, F. Atzeni, P. Sarzi-Puttini, M. Turiel, L.R. Lopez, M.T. Nurmohamed, Is atherosclerosis a autoimmune disease? *BMC Med.* 18 (12) (2014) 47.
- [26] N. Bassi, A. Ghirardello, L. Iaccarino, S. Zampieri, M.E. Rampudda, F. Atzeni,

- P. Sarzi-Puttini, Y. Shoenfeld, A. Doria, OxLDL/beta2GPI-anti-oxLDL/beta2GPI complex and atherosclerosis in SLE patients, *Autoimmun. Rev.* 7 (1) (2007) 52–58.
- [27] E. Matsuura, L.R. Lopez, Are Oxidized LDL/ $\beta$ 2-glycoprotein I complexes pathogenic antigens in autoimmune-mediated atherosclerosis? *Clin. Develop. Immunol.* 11 (2) (2004) 103–111.
- [28] K.P. Bliden, R. Chaudhary, L.R. Lopez, R. Damrongwatanasuk, K. Guyer, M.G. Gesheff, C.J. Franzese, H. Kaza, U.S. Tantry, P.A. Gurbel, Oxidized low-density lipoprotein-beta2-Glycoprotein I complex but not free oxidized LDL is associated with the presence and severity of coronary artery disease, *Am. J. Cardiol.* 118 (5) (2016) 673–678.
- [29] Z.G. Xia, M. Dickens, J. Raingeaud, R.J. Davis, M.E. Greenberg, Opposing effects of ERK and JNK-p38 MAP kinases on apoptosis, *Science (New York, N.Y.)* 270 (5240) (1995) 1326–1331.
- [30] B. Shishodia, B.B. Aggarwal, Nuclear factor-kappaB activation: a question of life or death, *J. Biochem. Mol. Biol.* 35 (1) (2002) 28–40.
- [31] Y. Zhao, C.X. Zhang, X.G. Wei, P. Li, Y. Cui, Y.H. Qin, X.Q. Wei, M.L. Jin, K. Kohama, Y. Gao, Heat shock protein 60 stimulates the migration of vascular smooth muscle cells via Toll-like receptor 4 and ERK MAPK activation, *Sci. Rep.* 19 (5) (2015) 15352.
- [32] R.M. Tombes, K.L. Auer, R. Mikkelsen, K. Valeri, M.P. Wymann, C.J. Marshall, M. McMahon, P. Dent, The mitogen-activated protein (MAP) kinase cascade can either stimulate or inhibit DNA synthesis in primary cultures of rat hepatocytes depending upon whether its activation is acute/phasic or chronic, *Biochem. J.* 15 (330) (1998) 1451–1460.
- [33] D. Bryk, W. Olejarz, D.Z. Downar, The role of oxidative stress and NADPH oxidase in the pathogenesis of atherosclerosis, *Postepy Hig. Med. Dosw.* 71 (0) (2017) 57–68.